People's Democratic Republic of Algeria

Ministry of Higher Education and Scientific Research

Larbi Tebessi University - Tebessa

Faculty of Science and Technology

Department of Mechanical Engineering

Presented for the purpose of obtaining a MASTER's degree

*Option: **Materials Engineering***

Theme :

Thermal modeling of rolling processes

Presented by: MEKHAZNIA RAHMA

In front of the jury

HANNACHI M^ed Tahar	**Professeur**	**Université Larbi Tébessi-Tébessa**	**Président**
Bouzid Al-Awadi	**M.C.B**	**Université Larbi Tébessi-Tébessa**	**Supervisor**
DIHA Abdellah	**M.C.A**	**Université Larbi Tébessi-Tébessa**	**Examiner**

Academic year. : 2022/2023


بسم الله الرحمن الرحيم

Thank you

First and foremost, we would like to thank God, our creator, who has given us the strength to complete this humble work.

This thesis could not have come to fruition without the contribution of many individuals, whom we now feel both happy and obligated to thank. First and foremost, we would like to thank the members of the examination committee for their cooperation during the review of this work and their participation in the defense. We would like to express our special gratitude to our supervisor, Dr. Bouzid Al-Awadi, for his guidance, advice, and assistance in this thesis. We also extend our gratitude to the professors of the Mechanical Engineering Department in general and the Materials Engineering Department in particular.

Finally, I would like to thank all those who directly or indirectly contributed to the preparation of this thesis. Here, I express my deep gratitude and respect.

I dedicate this humble thesis:

To my mother, who encouraged me to move forward and gave me all her love to pursue my studies.

To my father, who provided me with continuous support throughout my years of study.

To my brothers, Ghoulem, Housseme, and Ishak.

To my sisters, Bouthaina, Zoubida, and wissal

To all my friends without exception, especially chaima, Zanoubia,

and all my teachers: Dihah, Abdullah, Bouzid, Al-Awadi, Hanashi, Khalifa, and Lazhar Tarshan.

Abstract

The objective of this final year project is to analyze, in a general manner, the thermal phenomena occurring during the rolling process and to create a numerical model using the well-known finite difference method in the Matlab software to simulate these thermal phenomena accurately.

The choice of the modeling method for the rolling process depends on the nature of the problem being addressed (hot rolling, cold rolling).

The results of the thermal field obtained from the thermal model were compared to the results obtained from finite volume calculations using the Gambit and Fluent software.

ملخص

هدف هذا المشروع في السنة الأخيرة هو تحليل ظواهر الحرارة التي تحدث خلال عملية التدحرج وإنشاء نموذج عددي باستخدام طريقة الفروق المحدودة المعروفة في برنامج Matlab لمحاكاة هذه الظواهر الحرارية بدقة.

)اختيار طريقة النمذجة لعملية التدحرج يعتمد على طبيعة المشكلة التي يتم التعامل معها (التدحرج الساخن، التدحرج البارد. تمت مقارنة نتائج الحل الحراري الحاصلة من النموذج الحراري مع النتائج المستخرجة من حسابات حجوم محدودة باستخدام برامج Gambit و Fluent.

Résumé

L'objectif de ce projet de dernière année est d'analyser de manière générale les phénomènes thermiques se produisant pendant le processus de laminage et de créer un modèle numérique en utilisant la méthode bien connue des différences finies dans le logiciel Matlab pour simuler avec précision ces phénomènes thermiques.

Le choix de la méthode de modélisation pour le laminage dépend de la nature du problème abordé (laminage à chaud, laminage à froid).

Les résultats du champ thermique obtenus à partir du modèle thermique ont été comparés aux résultats obtenus à partir de calculs en volumes finis à l'aide des logiciels Gambit et Fluent.

SUMMARY

CHAPTER I

CHAPTER II

CHAPTER III

CHAPTER IV

LIST OF FIGURES

CHAPTER I :

CHAPTER II:

CHAPTER III:

CHAPTER IV :

General Introduction

In various industries, the concept of material forming plays a crucial role, whether in upstream, downstream, or in-production processes. The primary objective is to impart precise dimensions and mechanical characteristics to a metal component, within specified tolerance ranges. Among the most common forming techniques in the industry is rolling. This plastic deformation process, aimed at reducing the cross-section of a long product, involves passing it between two or more cylinders rotating around their axis. It is the rotation of the tools that drives the product through friction.

Rolling creates a deformation gradient along the thickness of the sheet. Shear deformation is more or less intense on the surface but absent at the mid-thickness of the sheet. The heterogeneity of mechanical properties leads to heterogeneity in the texture and microstructure of rolled products. These issues of heterogeneity and anisotropy in the mechanical properties of materials subjected to significant plastic deformation, as well as various heat treatments, are of crucial importance at the industrial level.

The main objective is to be able to predict, and even control, the mechanical characteristics and their variations across the thickness of the sheet. Commercially, it is the lower limit of the mechanical properties of the components that determines the accepted value for sale and serves as a reference for structural design. Above all, it is essential to identify the steps in the entire process, from cast material to the final product, that are decisive in the occurrence and/or control of heterogeneities. Therefore, understanding the conditions for the development of heterogeneities in mechanical properties and texture is paramount, as well as the development of a numerical procedure to predict them.

The forming process studied in this work is asymmetric rolling, which allows for reducing the thickness of a sheet (or product) by passing it between two cylinders with different diameters

(geometrical asymmetry) and/or rotating at different speeds (kinematic asymmetry) and/or having different surface states or temperatures. Asymmetry can also be caused by asymmetry in the properties of the incoming sheet, such as a temperature gradient between the top and bottom or differences in its rheological parameters.

Our contribution focuses on the thermal modeling of the rolling process, utilizing two methods: finite differences and finite volumes. Our work is structured into four chapters:

- The first chapter examines the theory of rolling.
- Chapter II presents a metallurgical study of rolling.
- In Chapter III, we present the thermal modeling of the asymmetric rolling process using finite differences and finite volumes, with a comparison of the obtained results.
- Finally, in Chapter IV, the thermal field results obtained using finite differences and finite volumes are compared.

CHAPTER I :

ROLLING THEORY

I.1. Definition

Rolling, as a highly diverse operation, can be summarized by the following definition: A plastic deformation forming operation aimed at reducing the cross-section of a long product by passing it between two or more axisymmetric tools rotating around their axis; it is the rotation of the tools that drives the product into the grip through friction.

As a fundamental operation in metallurgy, rolling accounts for approximately 90% of all metal production, encompassing all metals and alloys. Figure 1 provides some examples of rolling installations.

Rolling occurs after metal preparation, typically through continuous casting. Excluding a few "exotic" rolling processes (such as ring and wheel rolling, and return rolling of forged bars), rolling can be divided into:

- Rolling of long products (bars, wires, tubes, beams, rails), where both dimensions of the cross-section, usually of similar magnitude, are small compared to the length. The tools used are typically grooved cylinders (Figure 1a, b).
- Rolling of flat products (sheets, strips, and foils), where the thickness is small compared to the width, which itself is much smaller than the length. The tools used are almost cylindrical axisymmetric[2] objects (except for grinding curvature) (Figure 1c, d).

Rolling primarily provides semi-finished[1] products, with notable exceptions such as thick sheets, beams, and rails, as well as certain tubes. Other long products are intended for machining (bars), wire drawing (wire rod), and forging. As for flat products, they undergo metal shaping operations into sheets (such as stamping, fine cutting, spinning, and flow turning).

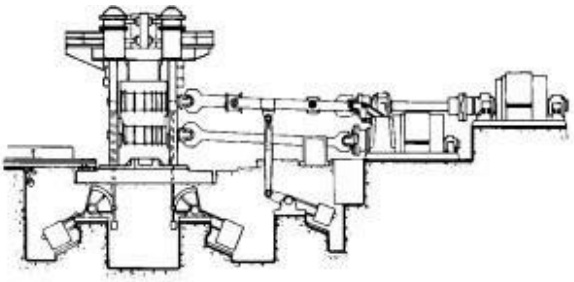

(a) laminoir à blooms (dégrossissage à chaud de produits longs)

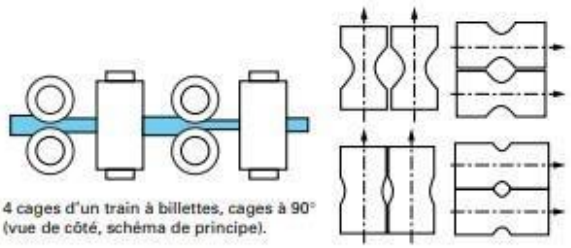

(b) laminage de produits longs : trains à billettes

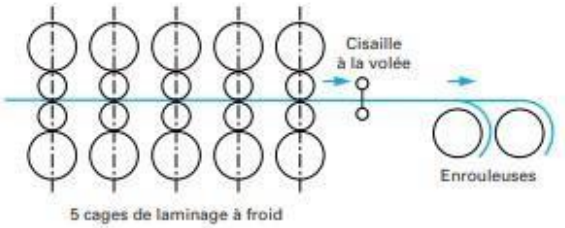

(c) laminage à froid de produits plats : schéma de principe d'un train tandem

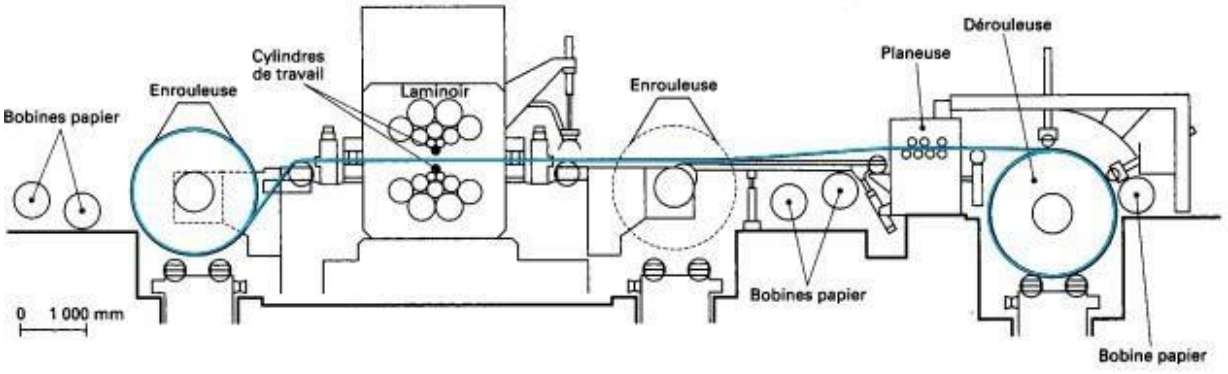

(d) laminoir Sendzimir, réversible à 20 cylindres, pour le laminage d'acier inoxydable (les bobines de papier sont destinées à protéger les surfaces brillantes)

Figure I.1. Some rolling plants

I.2. The terms "cold rolling" and "hot rolling"

are used in the context of material forming, specifically in controlled and repeatable shaping of materials. The process involves three types of controlled and repeatable properties:

1. Geometric shape with specific tolerances, which becomes more stringent.

2. Mechanical properties that require a suitable structural pattern.

3. Surface properties, primarily related to appearance and roughness.

Hot rolling starts when there is a need to work on a large section product, which enhances the economy in melting processes.[7] This requires significant deformation forces. Heating and softening the metal reduce these forces and the required equipment size, while providing the necessary ductility for extensive deformation. Many products, such as long products, thick sheets, and hot strips, undergo only hot rolling, followed by finishing operations such as heat treatments, tempering, pickling, coating, and machining.[5] Cold processes are generally necessary to achieve tight tolerances (around a few micrometers), high mechanical properties through increased stress, and good surface condition. Thin strips are almost exclusively cold-rolled.

For widely used alloys like steel and aluminum, it is noted that the hot rolling stage can be bypassed by casting thin slabs or melting thin strips. The cold rolling or hot rolling process generates differences for sure: we don't have the same temperature fields, and deep structural transformations (recovery, recrystallization, phase changes) occur at elevated temperatures but not in the cold. However, from a mechanical perspective, temperature only determines the stress levels. It does not significantly affect the deformation fields or stress rates, which are primarily governed by the plasticity of the material, precisely the ratio of deformed area dimensions (length L, width w, height h), contact locations, and free surfaces. Mechanically, the difference between hot and cold processes lies primarily in the product geometries they handle, more massive and "thicker" for the former and thinner for the latter. This is what drives the choice of one mathematical model over another, as we will see.

It should be distinguished between two directions for the terms "cold" and "hot." For the technical field, they simply refer to [3] whether we heat the product before rolling or not, to a temperature sufficient to reduce flow forces and increase ductility. In the field of metallurgy, the "hot" domain requires thermal activation of slip systems, which occurs when $T > 0.5\ T_{fusion}$ (in Kelvin). Therefore, lead, tin, and zinc are actually cold-rolled in their hot domains. The practical result is that they recrystallize upon cold rolling. Even aluminum, under excessive heating due to plastic deformation and friction, can reach this hot domain (around 200 degrees Celsius). Consequently, it can locally or completely recrystallize, with serious effects on process flow, microstructure, and mechanical properties, which becomes more painful as we approach the final product.

Therefore, cold rolling does not mean that we can get rid of thermal analysis. If thermal analysis is closely related to mechanics through metallurgy in the hot domain, it significantly affects corrosion reactions (through oil viscosity) in cold rolling. From a metallurgical perspective, some alloys are also heat-sensitive in the cold domain. Austenitic stainless steel exhibits a transition from austenite to martensite through cold deformation, which disappears if the temperature exceeds 100 degrees Celsius. Heating by plastic deformation is sufficient to prevent the transformation into martensite after the rolling process two or three times.[5]

I.2.1.Hot and cold rolling: differences and advantages

Steel, which is a variant of iron alloyed with carbon, often has other elements added to prepare it for industrial transformation and use. One of these elements is cold or hot rolling, which is a highly popular process that prepares steel for use. It is widely used in the tube industry.[2]

Rolling is an industrial metal forming process in which a metallic material is introduced between one or more pairs of rolls to reduce its thickness and make it more uniform. It is a process similar to rolling a rolling pin over pizza dough, and its objective is to enhance the mechanical properties (tensile strength, yield strength, elongation, etc.) of the material.

Rolling is classified based on the temperature of the rolled material. It can be either hot or cold rolling.

Therefore, there will be many cases where a coupled thermo-mechanical model will be necessary.

I.3. Steady State and Transient Phases

Most rolling operations exhibit a dominant or even exclusive steady-state regime. However, transient phases still exist, such as the head and tail of a plate, sheet, slab, or strip, and the weld between coils in continuous cold steel rolling. Additionally, considering the thermal regime as steady-state, especially for cylinders, is very difficult. Models, for the sake of computational time efficiency, often focus on the steady-state regime unless the problem under study is precisely related to transients, which unfortunately is often the case.

Rolling mill vibrations are one of the most concerning issues today, exacerbated by the increase in rolling speed. In particular, the phenomenon known as "chatter" is a vibration with a frequency of 100 to 200 Hz that forces the operator to reduce the speed. Excited by any fluctuation in input parameters, as long as the rolling speed gives it a frequency in that range, chatter is self-sustaining due to the phase quadrature between the vertical vibrations of the working rolls and the consequent fluctuation of strip tensions [1] (Figure 2). Anything that increases the effect of strip tensions on the rolling force contributes to destabilization (such as rolling with reduced thickness due to roll deformation [see M 3 066]; low friction, approaching the slip limit, negative or quasi-zero forward slip).

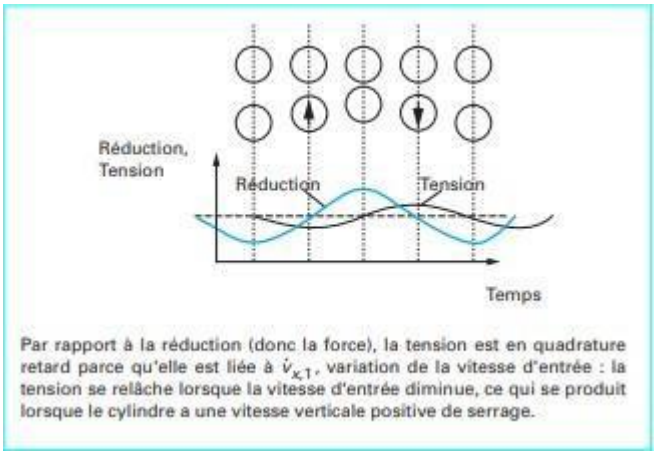

Figure I.2. Source of browsing

I.4. Rolling Defects

Just as we have distinguished three levels of imperatives (geometric, microstructural, and surface), we will have three families of problems or defects.

■ Geometric defects (Figure 3) (products out of tolerance): Metal flow is never completely confined, as the tools would suffer too much. This leads to "competitions" between different types of flow, such as spreading, which competes with elongation of the product (Figure 3a, b). Therefore, the ends of long products, as well as the ends and edges of flat products, are always deformed (Figure 3c, d) and require cropping (their sum constitutes the trim). Furthermore, the machines (rolls) and tools (cylinders, rollers), which are not infinitely rigid, yield elastically under the applied hundreds of tons. This also disrupts the geometry of the products, creating profile issues (Figure 3e) and flatness problems (Figure 3f) for flat products (transverse thickness variations and deviation from the average surface flatness of the sheet or strip). Finally, problems with the adjustment of production tools can have similar consequences (a misalignment of rolls causes a "sword" defect: Figure 3g, while asymmetry in diameter, speed, or friction between top and bottom results in a "ski" defect: Figure 3h...).

■ Microstructural defects: These defects are numerous and highly dependent on the alloy considered but not specific to rolling. They include inappropriate or heterogeneous grain sizes, misoriented or excessive textures (crystallographic, morphological, or topological), excessive or insufficient non-metallic inclusions, porosity, cracks, or fissures. Some of these defects are inherited from casting structures [17], and the challenge is to design a tolerant rolling process or, better yet, capable of resolving them. Others are created during rolling due to critical temperatures, deformation states, and dangerous stresses (cracks): the process must be designed to avoid them.

■ Surface defects: This category encompasses defects that impair the product's subsequent use, along with others that only cause aesthetic inconvenience (the human eye is highly sensitive to visual inconsistencies, and the surface is the visible part of a product!). We can

distinguish defects of a chemical nature (segregation, and more often pollution: carbon stains resulting from annealing of sheets due to lubricant cracking, etc.), as well as inadequate roughness. Note that for stamping sheets, in particular, but also for chemical etching, specific morphology of peaks and valleys is required, not just a certain level of roughness as in the past ("Ra"). The risks of defects and non-conformity increase accordingly.

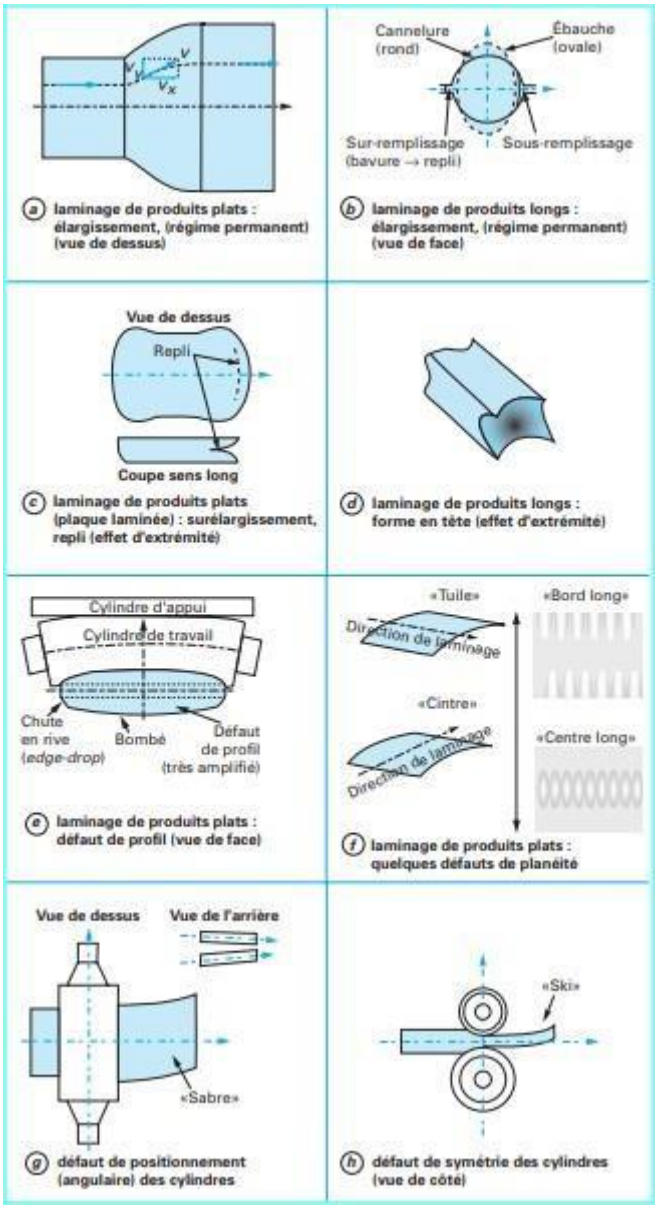

a laminage de produits plats : élargissement, (régime permanent) (vue de dessus)
b laminage de produits longs : élargissement, (régime permanent) (vue de face)
c laminage de produits plats (plaque laminée) : surélargissement, repli (effet d'extrémité)
d laminage de produits longs : forme en tête (effet d'extrémité)
e laminage de produits plats : défaut de profil (vue de face)
f laminage de produits plats : quelques défauts de planéité
g défaut de positionnement (angulaire) des cylindres
h défaut de symétrie des cylindres (vue de côté)

Figure I .3.Some rolling problems or defects

I.5.Thermal Models

Rolling presents a wide range of thermal problems. It starts with the reheating furnaces for hot rolling, where the temperature homogeneity must be ensured while minimizing energy usage. The goal is to achieve a homogeneous temperature for the product to be rolled, which should be as consistent as possible from one slab to another. Prolonged contact of the hot metal with the roller tables can create detrimental cold spots during rolling and affect [10]the properties of the final product. The thermal behavior at the interface between the product and the tool is particularly delicate, as it involves high-

pressure contacts with strong heat exchange. Consequently, the product's surface undergoes significant thermal cycles that impact its microstructure (including the behavior of the oxide layer, such as mill scale in the case of steel). The cylinder also experiences thermoelastic stress cycles, which contribute to cracking (known as "faïençage") and oxidation, damaging the product's surface, especially for high-temperature alloys like steel. Therefore, thermal considerations involve a coupled analysis of the product and the tool. Additionally, there[9] is the unique thermomechanics involved in scale removal from steel (using high-pressure water jets following slight rolling passes), as well as controlled cooling after hot rolling, which can induce deformations and residual stresses due to phase transitions (in rails, beams, thick sheets), requiring straightening or leveling. In the cold rolling mill, thermal effects at the interface are influential in terms of lubrication and friction, and in continuous annealing furnaces, precise thermal histories are essential to achieve the desired microstructure and mechanical properties.

While leaving the discussion of furnace models to others, [11]we will focus on the rolling and cooling phases. For these, the finite difference method is often used if gradients in two or three directions need to be considered. Otherwise, if only the average temperature in the section is of interest, the slice method has its thermal counterpart. [7]The resulting equation will take into account the heat losses through radiation, natural or forced convection, contact with the tables, as well as any internal heat sources (latent heat of phase transition). For the interface, the internal source of plastic deformation and the surface source of frictional dissipation are explicitly considered.

I 2.The Rolling Mill

A rolling mill is a machine used in the metallurgical industry to reduce the thickness and modify the shape of metal materials such as ingots, slabs, or plates. It is primarily used in the production of sheets, plates, bars, wires, and other rolled metal products.

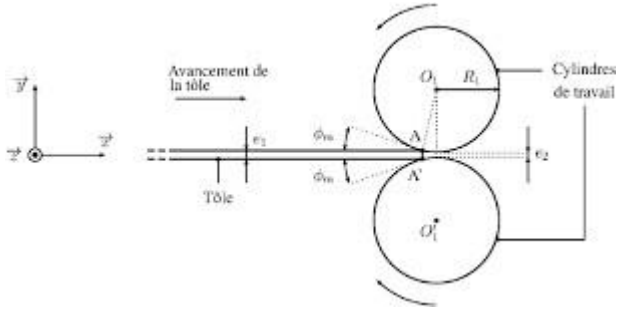

Figure I.4.pricipal of operation of rolling mill cylinder.[10]

The rolling process in a rolling mill typically takes place in several stages. Firstly, the metal material [4]is heated to an appropriate temperature to make it more malleable. Then, the material is introduced between two rotating rolls (or cylinders) that apply pressure to the aterial and gradually compress it.

The rolling mill can have different configurations depending on the desired end products. For example, it can be a hot rolling mill used for high-temperature rolling, or a cold rolling mill used for rolling at room temperature. There are also reversible mills where the rolls can rotate in both directions, and multi-roll mills to achieve specific shapes and thicknesses.[5]

The rolling mill is usually equipped with cooling systems to prevent overheating of the rolls, as well as adjustment mechanisms to control the thickness of the rolled material. It may also be accompanied by other equipment such as shears for cutting the material into sheets or strips, and coilers for winding the finished products.

The rolling process in a rolling mill allows for the production of metal products with specific dimensions and mechanical properties. It is an essential step in the manufacturing of many metal products used in various industrial sectors such as automotive, construction, aerospace, etc.[14]

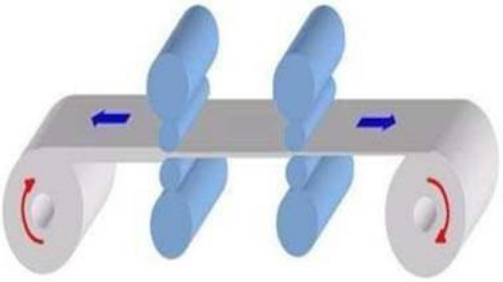

Figure I.5.Rolling Train [9]

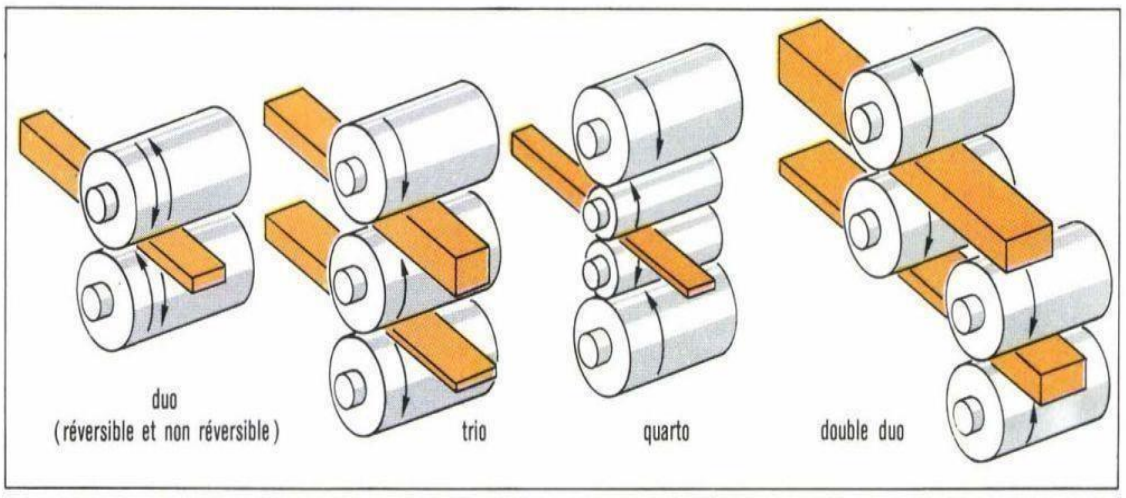

FigureI.6.differnts types of rolling mills [14]

I.6.1.Quarto rolling

In a quarto rolling mill, the slab is rolled through two quarto stands (consisting of four cylinders), a roughing stand and a finishing stand, until the desired thickness is achieved. The resulting plate is then cooled and leveled. This technique allows for the rolling of wider and/or thicker plates compared to a hot strip mill, and depending on the required quality, the mechanical properties of the quarto plate are often improved through heat treatments such as normalization. The EN 10029 standard specifies tolerances on the dimensions and shape of the quarto plate.

The mill stands in quarto rolling mills are typically composed of two small-diameter work rolls (around 10 cm) for rolling and two larger-diameter backup rolls, as schematically shown in Figure I.8. Various actuators in the mill stand, such as clamping screws, hydraulic cylinders, etc., are used to adjust the correct thickness at the exit of the mill stand.

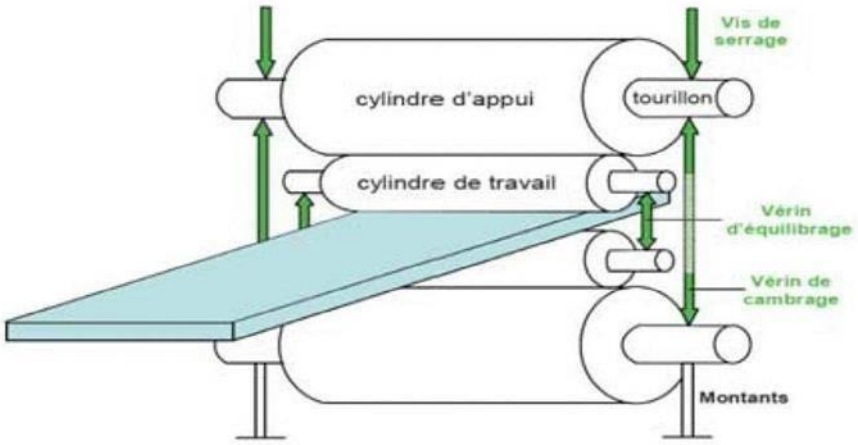

Figure I.7.Diagram of a quarto rolling cage[3].

I.3.Rolled products

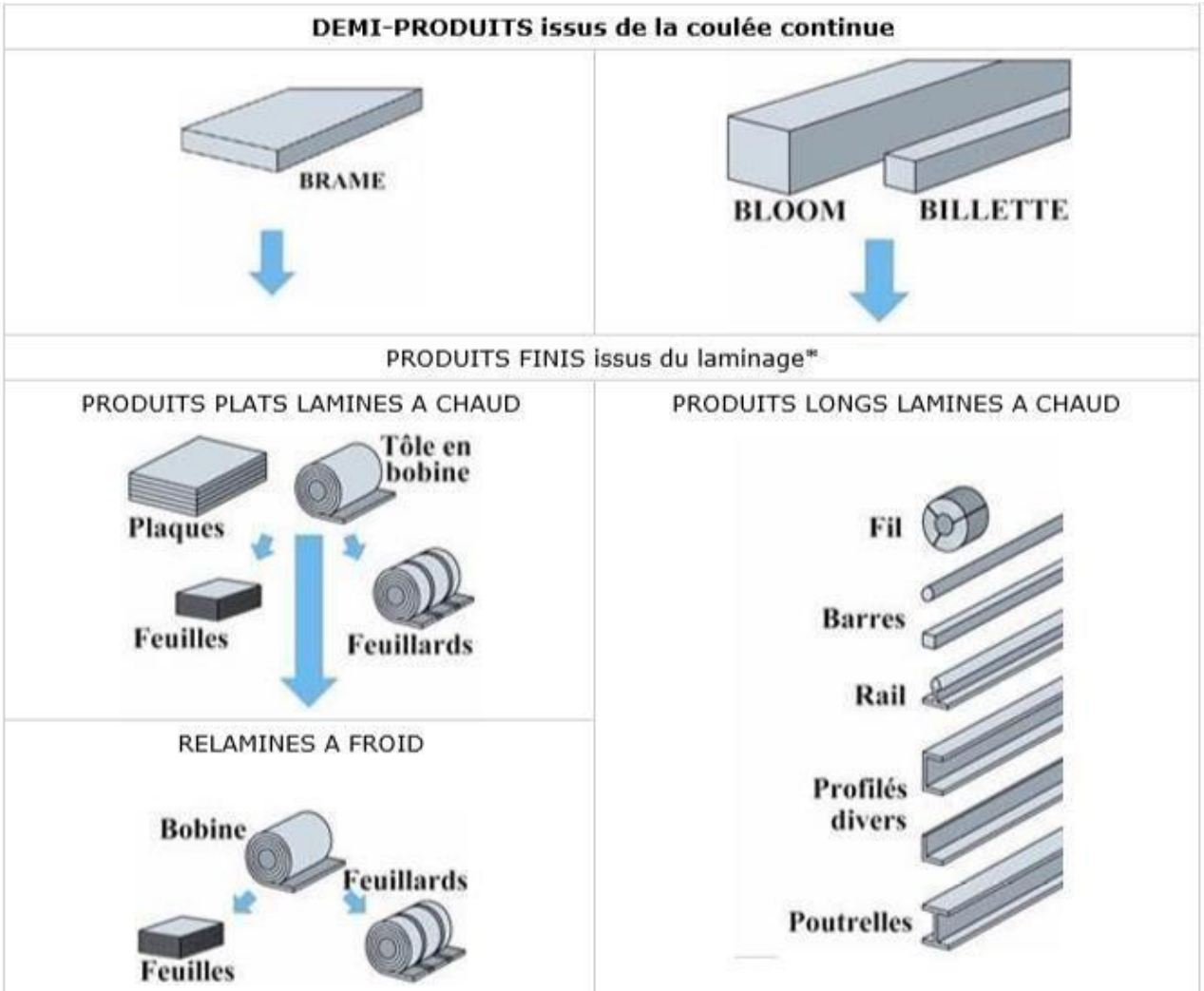

Figure 1.8.Rolling product [12]

CHAPTER II: HOT ROLLING METALLURGY

II.1. Some reminders about steels

As a preliminary note, it is important to recall the main specificity of steel compared to many other metallic materials, which is that its crystallographic structure changes with temperature as shown in the Fe-C phase diagram in Figure 1.

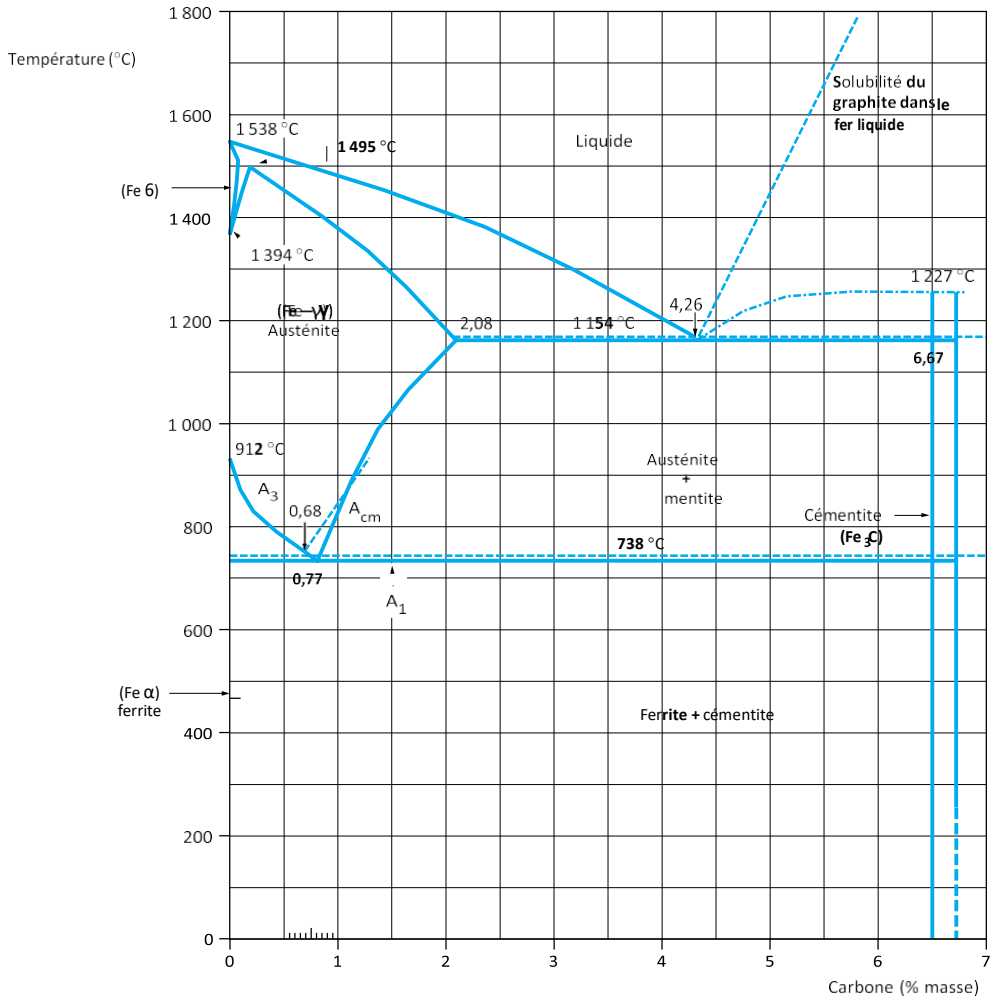

Figure II.1: iron-carbon equilibrium diagram

In the case of conventional steels, we can schematize these solid-solid phase transitions as follows:

- At high temperatures (T > Ae3), the crystallographic structure is of the face-centered cubic type, and as it is a single phase called austenite, we refer to it as the austenitic structure, phase, or austenitic domain (or γ).
- At low temperatures (T < Ae1), the structure is of the body-centered cubic type. In this case, several phases with this crystallography can coexist: ferrite, cementite, and perlite (ferrite + cementite eutectoid) for equilibrium phases, and bainite, martensite, and residual austenite

for non-equilibrium phases.

We will then refer to the α phase and, colloquially, to the ferritic phase.

- At intermediate temperatures, the structure is a mixture of austenitic phase and α phase (usually ferrite), with the respective proportions of the phases determined by the temperature and the steel's chemistry. This is in the intercritical domain.

Note

- Ae1 is the equilibrium temperature defining the lower limit of the austenite existence domain.
- Ae3 is the equilibrium temperature defining the upper limit of the ferrite existence domain.

In practice, for most steel products, the hot forming phase is carried out in the austenitic domain (although in specific cases, there may be an intention to finish rolling in the intercritical or even fully ferritic domain). During cooling after exiting the rolling mill, the steel will gradually transition from the γ phase to the α phase.

We will subsequently see how cooling conditions, the chemical composition of the steel, and the structural state of the austenite prior to the γ/α transformation influence the α structure in terms of the nature, fraction, and size of the phases, and consequently, the final mechanical characteristics. It should be kept in mind that the existence of this allotropic transformation represents a significant means of control over the final product, provided that the metallurgical tools are appropriately adapted.

The second important metallurgical point concerns the ability of certain metallic elements present in steels (such as Nb, Ti, V, Al...) to precipitate by associating with non-metallic elements (N, C, S...). Indeed, the solubility of the alloying elements in pure iron matrix depends on the content of these elements, temperature, and crystallographic structure. Once the solubility limit is reached, and if the diffusion kinetics is sufficiently fast, precipitation will occur.

Example

We can cite the precipitation of titanium nitrides (TiN), aluminum nitrides (AIN), niobium carbonitrides (Nb(C, N)), titanium carbides (TiC)... These precipitates can harden steel at room temperature when they are numerous and/or fine enough (< 1 mm). This is one of the reasons why niobium, titanium, and vanadium are added to steels that need to have fairly high mechanical characteristics.

The second objective, which is rather a beneficial consequence of the first, is to position oneself in the austenitic domain, resulting in partially erasing the coarse structure resulting from solidification and reducing the composition gradients caused by the segregation phenomenon.

Finally, the main objective of this heating phase is to put back into solution the precipitates that appeared during solidification. Firstly, because they are too large and therefore not numerous enough to contribute to the hardening of steel at room temperature. Secondly, considering that elements such as niobium, titanium, or vanadium play a crucial role in the evolution of the structure during rolling and allotrope transformation when they are in a solid solution. We will also see that the dissolution of the precipitates has an important effect on the size of the austenitic reheating grain.

II.1.1. Hot rolling involves several phases

In this paragraph, we will describe the different phases of hot rolling and the physical mechanisms involved after presenting the characteristics of the initial product, whether it is a slab or a billet.

II.1.2. Characteristics of the initial product

We deliberately consider the case of cold or warm charging (T < Ae3). In accordance with metallurgical reminders.

The second objective, which is rather a favorable consequence of the first one, is to place oneself in the austenitic domain, with as consequences, partially erasing the very coarse structure resulting from solidification and reducing the composition gradients due to the segregation phenomenon.

Finally, the essential objective of this heating phase is to put back into solution the precipitates that appeared during solidification, first because they are too large and therefore not numerous enough to contribute to the hardening of the steel at room temperature, and because elements such as niobium, titanium or vanadium play a very important role in the evolution of the structure during rolling and allotropical transformation when they are in solid solution.

We will also see that the dissolution of the precipitates has a significant effect on the size of the austenitic reheating grain.

II.2. Reheating

Reheating carbon steels and microalloyed steels has three main objectives.

The first, of a mechanical nature, is simply to raise the metal to a sufficient temperature to reduce forming stresses, increase the ductility of the steel in order to apply significant deformations to it, and to finish rolling in the austenitic domain.From these equations and the content of the elements, it is easy to calculate the solubility temperature of the considered precipitate. Conversely, it is possible to calculate, at a given temperature, the quantity of respective elements in solid solution.

II.2.1. Putting precipitates back into solution

The redissolution of precipitates is such an important objective that reheating temperatures are often set to achieve near-complete or complete redissolution of the metallic elements.

For example, in the case of flat products, the reheating temperature is typically around 1150 to 1180°C for a C-Mn steel as it is sufficient to redissolve the aluminum nitrides (AIN), which are the only precipitates, present in these steels. On the other hand, reheating of niobium microalloyed steels is conventionally carried out above 1220°C to dissolve the niobium carbonitrides (Nb(C,N)).

Numerous authors [1] [2] [3] have determined the redissolution laws for the main precipitates present in steels, at least when only one analytical population of precipitates is present. These laws are expressed by an equation of the following form:

Where [M] and [X] represent the mass fractions (%) of the metallic element and the non-metallic element, respectively.

$$lg[M][X] = -\frac{A}{T} + B$$

A et B constantes,
T : température °(K).

Among the most well-known ones, we can mention Gladman's redissolution law for aluminum nitrides [1].

$$lg[Al][N] = -\frac{6770}{T} + 1{,}03$$

with T temperature (K).

Using these equations and the content of the elements, it is straightforward to calculate the temperature at which the considered precipitate is completely redissolved. Conversely, it is possible to calculate, at a given temperature, the quantity of respective elements in solid solution.

Example

For a steel with 0.04% aluminum and 0.007% nitrogen, the temperature for complete redissolution of aluminum nitride (AlN) is 1204°C.

II.2.2 Grain Growth at Reheating

One of the metallurgical consequences of precipitate dissolution is grain growth during reheating. During austenitization (T > Ac3), austenitic grains that form at the former ferritic grain boundaries tend to grow due to the elevated temperature. However, the driving force for this growth is

relatively low, and the precipitates resulting from solidification, even if coarse and therefore few in number, impede the movement of new grain boundaries. As the precipitates dissolve, the boundaries regain their mobility, allowing the grains to grow. These phenomena can be observed in Figure 4 for steels 1 and 2 containing dispersoid elements, where regions of rapid grain size growth are visible.

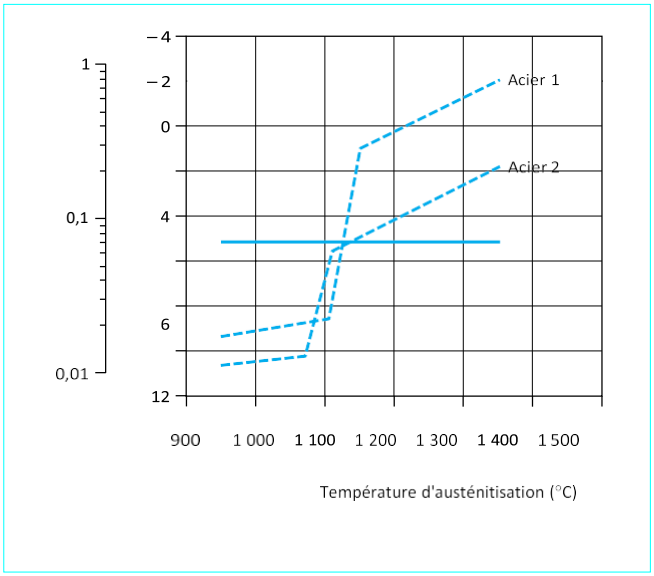

Figure II.2: Change in austenitic grain size as a function of reheating temperature [36]

They occur in temperature ranges corresponding to partial precipitate dissolution, where fine grains that are still blocked by precipitates coexist with larger grains that have grown freely. It is desirable to operate outside of these temperature ranges characterized by heterogeneous structures while maintaining moderate temperatures to limit grain coarsening. Note: Ac3 is the temperature at which ferrite completes its transformation into austenite during slow heating.

II.3. Rolling

From the metallurgist's perspective, rolling itself is merely a sequence of deformations (passes) that result in work hardening of the metal, with intermittent waiting periods (inter-passes) during which the steel's structure can evolve. First, we will describe the phenomenon of work hardening and the different mechanisms involved in "combating" this non-equilibrium state.

II.3.1. Work Hardening and Metal Restoration during Deformation

The elastic deformation of any crystalline material occurs through reversible distortion of its lattice. This phenomenon has a limited range, and when the imposed deformation exceeds a critical deformation - the yield point - the mechanisms involved at the microscopic scale to accommodate the applied macroscopic deformation differ. Deformation then occurs through breaking and

rearrangement of the metallic bonds that maintain the continuity of the crystalline lattice, phenomena that theoretically require considerable energy. Fortunately, crystalline lattices are "imperfect," meaning they contain defects in atomic arrangement known as dislocations. The presence of these linear defects and their displacement along preferred planes allows for discrete breaking and rearrangement of the bonds, reducing the required energy significantly.

In a non-deformed metallic material (at equilibrium), the density of these defects is already significant (approximately 10^10 to 10^11 dislocations/m^2 at room temperature). However, their number rapidly increases with plastic deformation, leading to the hardening of the steel; this is the phenomenon of work hardening. It is evident that this mechanism has limits, particularly in ensuring the integrity of the crystalline network. Various mechanisms are employed to counteract the creation of new dislocations, leading to their elimination and thus the softening of the material. These mechanisms are known as restoration and recrystallization.

The objective of this text is not to provide a detailed microscopic description of these phenomena, for which references [4] [5] should be consulted. However, to differentiate between these two softening mechanisms, we use the term restoration when the elimination of dislocations occurs discretely without significant alteration of the metallurgical structure, and recrystallization when the creation of new grains and the movement of grain boundaries are involved, leading to simultaneous elimination of a large number of dislocations. It is also necessary to distinguish between softening that occurs concurrently with deformation and that which occurs after deformation during inter-pass times. In the former case, we refer to it as dynamic restoration or recrystallization, while in the latter case, it is static restoration and recrystallization (Figure 5). The microscopic mechanisms involved in both situations are similar, but the resulting consequences on the metallurgical structure can differ, particularly with regard to recrystallization.

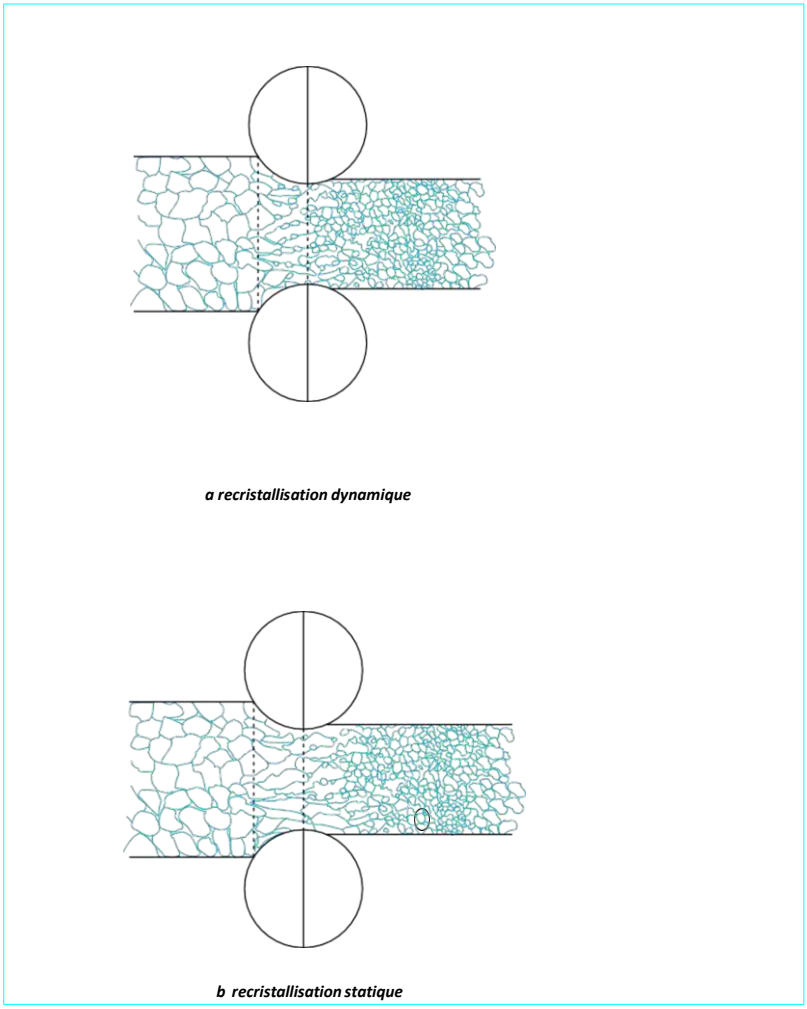

Figure II.3: Dynamic and Static Recrystallization

To accommodate the applied macroscopic deformation, dislocations move along preferred slip planes. Since the number of these planes is limited (typically 4 to 5 at most), there is a significant probability for two dislocations of opposite signs to move on the same slip plane, resulting in their respective elimination. The second mechanism involved in restoration is recrystallization, which involves the rearrangement of dislocations into boundaries that define subgrains. The higher the temperature, the more favorable diffusion phenomena become, leading to faster softening through these mechanisms.

In contrast to recrystallization, it is important to note that dynamic restoration occurs as soon as deformation is applied. This explains why a metal is softer at high temperatures than at room temperature, as the dislocations generated by deformation are partially eliminated at high temperatures through restoration.

II.3.2. Recrystallization

For certain materials , restoration is not sufficiently effective in terms of reducing work hardening. Softening then occurs through the nucleation and growth of new grains, leading to a much faster elimination of dislocations. The heavily elongated, work-hardened grains are gradually replaced by new equiaxed grains. Whether it is recrystallization or allotropic transformation, the preferential sites for nucleation of new metallurgical grains are grain boundaries. They provide efficient diffusion paths and, in the case of recrystallization, act as areas of work hardening accumulation. Although work hardening may appear homogeneous on a macroscopic scale, it is actually highly heterogeneous on a microscopic scale. In the case of static recrystallization, when a high applied deformation rate is present, nucleation can also occur within the grain (intragranular).

Of these two phenomena, only recrystallization generates a significant modification of the metallurgical structure. Therefore, the thermomechanical treatment of steels largely focuses on exploiting this mechanism during rolling. That's why we will exclusively discuss the consequences of this mechanism on the structural evolution of steel. We will examine the parameters that determine the prevalence of one mechanism over the others.

II.3.3. Static Recrystallization

Static recrystallization is the preferred mode of structural evolution in steels during shaping at high temperatures. Consequently, it has been fairly comprehensively studied in terms of mechanisms, kinetics, and structural consequences [6] [7] [8] [9]. The effect of thermomechanical parameters and the chemical composition of the steel are described in the following paragraphs.

II.3.3.1. Specifics of Static Recrystallization Phenomenon

As mentioned earlier, recrystallization occurs through the nucleation and growth of new grains. Complete recrystallization is achieved when the work-hardened grains have been entirely eliminated and replaced by equiaxed grains. Except in exceptional cases, the grain size at the end of recrystallization is finer than the initial grain size.

Since static recrystallization occurs after the cessation of deformation, its kinetics are expressed in terms of time. It exhibits a specific behavior (Figure 6) that can be well described by an Avrami-type law:

$$\boldsymbol{FR(t) = 1 - \exp(kt^{n})}$$

with FR :static recrystallization rate,

t : time,

k and n : two constants characterizing the kinetics.(n=2 ά 5)

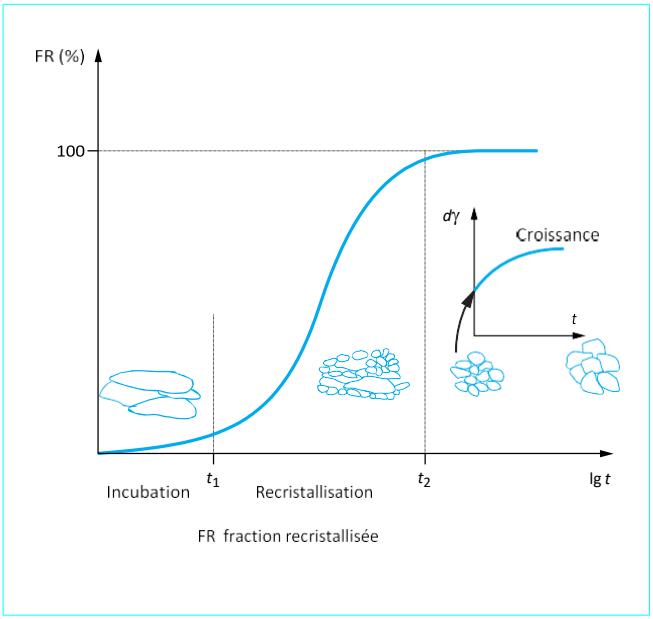

Figure II.3 : Static recrystallization kinetics

In this figure, we observe the existence of an incubation time, which can be associated with the germination phase, and strongly depends on the thermo-mechanical parameters and chemical composition of the steel. These same parameters also have a considerable influence on the growth phase of recrystallized grains, as visualized by the slope of the kinetic law curve.

II.4. Effect of Thermo-mechanical Parameters on Static Recrystallization Kinetics and the Structure at the End of Recrystallization

The two predominant thermo-mechanical parameters in terms of static recrystallization are the deformation rate and the temperature. We will also discuss the effect of the deformation rate.

■ Effect of the deformation rate

The higher the applied deformation, the greater the stored energy in the structure, and the higher the driving force for recrystallization. This results in an acceleration of kinetics (Figure 7a) in terms of germination (shorter incubation time) and grain growth (steeper slope of the curve). However, it should be noted that there is a critical deformation rate below which no recrystallization occurs. Studies published by different research teams indicate that this critical deformation is around 5 to 7%.

Regarding the grain size at the end of recrystallization, the higher the applied deformation rate, the greater the number of germination sites. Consequently, the size of recrystallized grain decreases as deformation increases (Figure 8).

■ **Effect of temperature**

Two antagonistic phenomena are associated with the effect of temperature. On one hand, at a constant deformation rate, the higher the temperature, the lower the work hardening of the structure upon deformation cessation due to more extensive restoration.

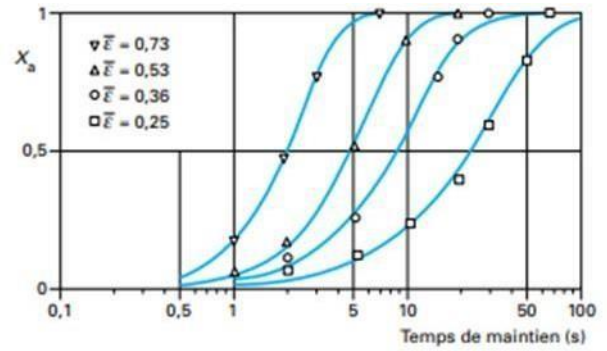

ⓐ **effet de la déformation sur les cinétiques de recristallisation statique**

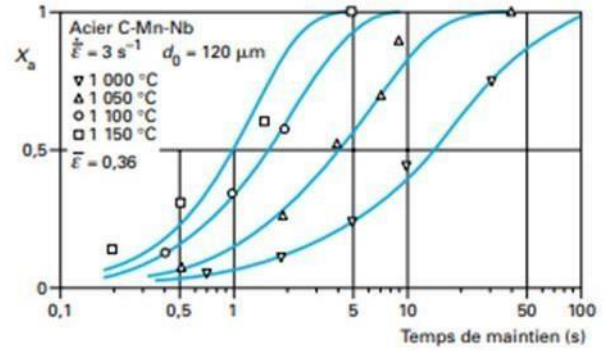

ⓑ **effet de la température sur les cinétiques de recristallisation statique**

X_a taux d'adoucissement (équivalent au taux de recristallisation)
$\bar{\varepsilon}$ déformation équivalente
d_0 taille du grain austénitique de réchauffage
$\dot{\bar{\varepsilon}}$ vitesse de déformation

Figure II.4 : Static recrystallization kinetics

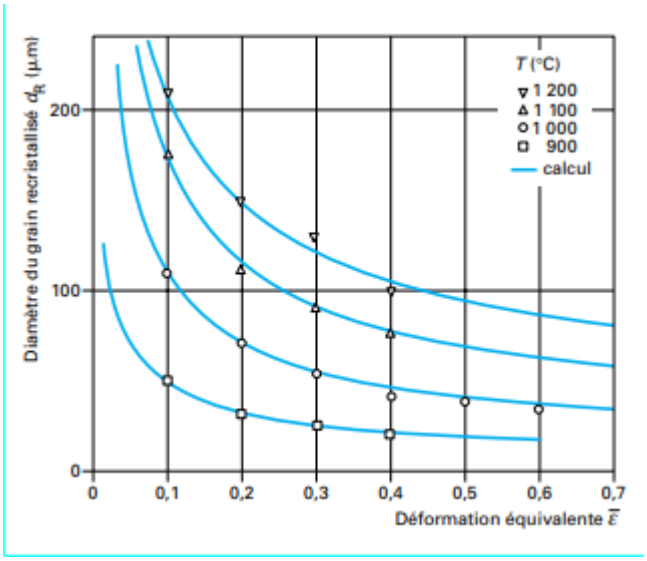

Figure II.5: Effect of deformation and temperature on recrystallized grain size

with, as a consequence, a presumably lower driving force (cf. previous paragraph). However, the considerable effect of temperature on diffusion phenomena accelerates the growth of newly recrystallized grains and, therefore, the kinetics. Figure 7b demonstrates that the second effect is largely predominant.

The higher the temperature, the larger the recrystallized grain (Figure 8). This is the consequence of the two phenomena described above: the higher the temperature, the lower the work hardening at the end of deformation, resulting in fewer nucleation sites for new grains. Additionally, the higher the temperature, the faster the growth of new grains.

■ **Effect of the deformation rate**

This parameter has a limited effect on static recrystallization. A higher deformation rate slightly accelerates the kinetics. This is due to increased work hardening at a given deformation rate. For the same reason, the size of the recrystallized grain is slightly finer.

We have just reviewed the effect of thermo-mechanical parameters on static recrystallization. Now we will study the influence of the steel's chemical composition.

II.4.1.Effect of Chemical Composition on Static Recrystallization Kinetics and Grain Size at the End of Recrystallization

The effect of the chemical composition of steels on recrystallization has been studied quite extensively [7] [9]. In this paragraph, we will "focus" on the effect of microalloying elements, particularly niobium, which will help us understand its essential role.

Most solid solution elements have an influence on recrystallization kinetics, which is often associated with the modification of diffusion conditions and the slowing down or inhibition of dislocation or grain

boundary movement. This effect is particularly significant when microalloying elements precipitate concomitantly with recrystallization.

Figure 9 a (adapted from [7]) shows the relative influence of chromium, nickel, manganese, and molybdenum. The apparent effects are relatively small even for contents ranging from 1 to 2%, except for molybdenum, which induces a significant increase in the incubation time. The influence of microalloying elements (titanium, vanadium, and niobium) is visualized in Figure 9b (adapted from [7]). Their effect is considerable considering the quantities involved (approximately 0.1%), as recrystallization times are multiplied by 10 or even 1,000 compared to carbon steel (i.e., without microalloying elements), especially in the case of niobium. It is evident that, given the short inter-pass times typical of rolling processes (cf. § 2), the presence of this element can even inhibit static recrystallization. A judicious use of niobium will thus allow for control of the structural evolution of steel during rolling and, consequently, control of the structure and final properties of the product (it should also be noted that this element contributes to final hardening by precipitating as carbides and carbonitrides during coiling). Figure 9 c further shows that the niobium content accentuates its action on recrystallization.

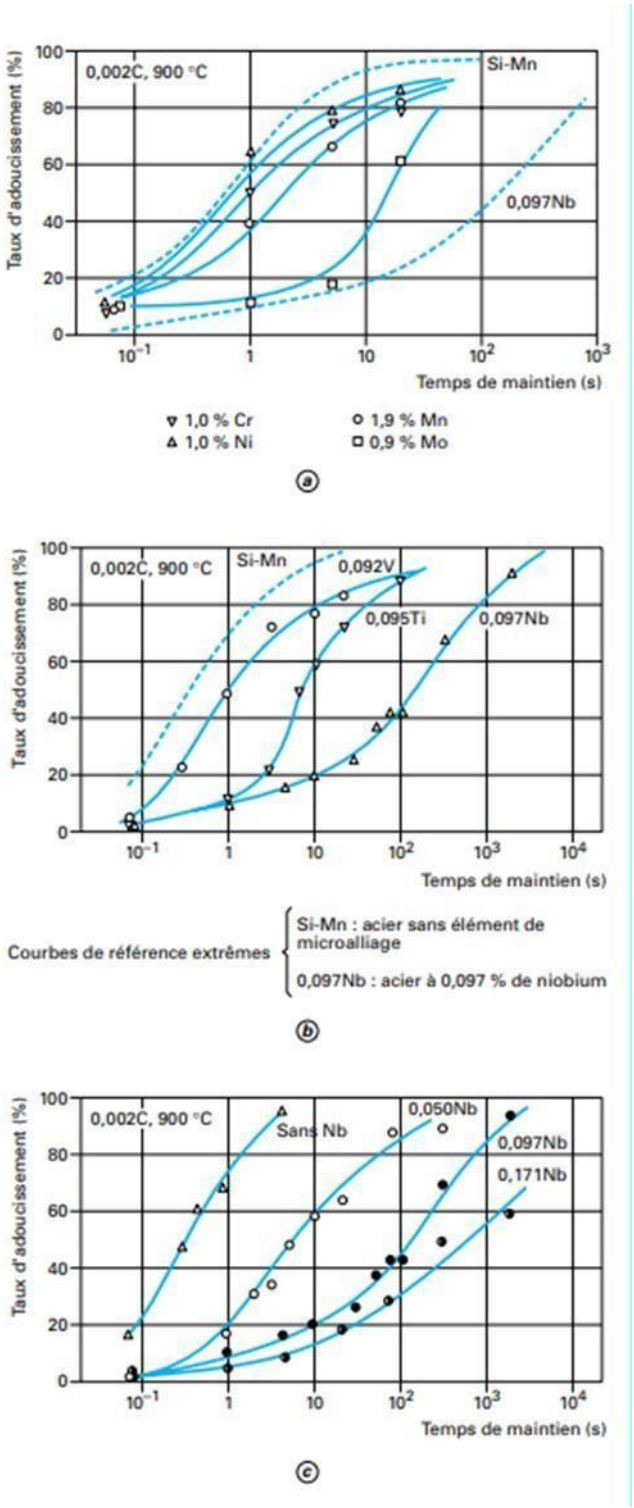

Figure II.6: Influence of micro alloy elements on static recrystallization kinetics

CHAPTER III: RESOLUTION METHOD

III .1.Consideration of thermal aspects

In general, all thermal modeling work relies on the classical equation of energy conservation, known as the "heat equation," which is written in its most general form as follows:

$$\rho c^{p} \frac{\partial T}{\partial t} + \rho c^{p} \vec{u}.\vec{grad}T = div(\lambda \vec{grad}T) + \dot{w}^{voL} \quad \text{(III.1)}$$

T represents the temperature field.

ρ is the density expressed in kg.m^(-3).

C^{p} is the specific heat capacity expressed in $J.kg.k^{-1}$.

$\vec{u}$ is the velocity field.

$\dot{w}^{voL}$ represents any volumetric heat sources.

The convective term $\vec{u}.\vec{grad}T$ must be taken into account in Eulerian calculations, which can be useful for rolling processes where the material flows through the rollers while the center remains at a fixed position. Generally, ρ, C^{p}, and λ are considered as constants, although they may depend on temperature.[1]

III.1.2.a Surface heat sources

Heat sources are specifically considered as imposed heat fluxes of the Fourier type. They are often located at [11]the tool/material interface and are formalized as follows:

$$-\lambda \vec{grad}T.\vec{n} = \Phi^{d} \quad \text{(III.2)}$$

Where Φ^{d} is the imposed surface heat flux and $\vec{n}$ is the outward normal to the material at the contact surface. Φ^{d} can represent various phenomena depending on the authors.

Surface heat flux: It can represent the surface heat flux as a part of the frictional energy. The heat generated by friction between the cylinders and the sheet is shared both in the material and in the tools. Therefore, even if the model does not consider the cylinders, a partition coefficient must be introduced to quantify the amount of heat propagating only in the sheet. For this purpose, [Baque et al., 1973] introduce the effusivity, $e = \sqrt{(\rho\ C^{p}\ \lambda)}$, and thus the boundary condition becomes:

$$\Phi^{d} = \frac{e^{matie\ e}}{e^{matier e} + e^{matier e}} \quad \text{(III.3)}$$

This expression of the partition coefficient was established within the framework of a one-dimensional thermal problem for two semi-infinite bodies with constant thermal properties. This

expression can then provide an indicative value of the heat transfer coefficient between the tool and the plates. [9]

III.1.3.b Heat dissipated by plastic deformation

Assuming that the flow stress σ_0 is constant during deformation and $\bar{\varepsilon}$ is the deformation experienced by a material element of volume V.

The plastic deformation energy dissipated in the material is $\sigma_0 \dot{\bar{\varepsilon}} V$. This dissipation corresponds to an increase in internal energy.

Let ρ be its volumetric mass and c be the specific heat. It is observed that only a fraction of the deformation power is used for heating the material. The rest is used as work hardening energy. The expression for the plastic energy transformed into heat is given by the equation:

$$\dot{W}_{vol} = \Gamma^{d} \sigma_0 \dot{\bar{\varepsilon}} \quad \text{(III.4)}$$

Where ^{d} can be approximated as the Taylor-Quinney coefficient. It is typically close to 0.9 (see Table I.1). Moreover, for the majority of metals, its exact value is not known.[10]

Métal	Γ_d
Cuivre	0.92
Aluminium	0.92
Acier doux	0.87

Table III.1 Taylor Quinney coefficient for different materials [1]

Establishing this heat source also requires coupling the thermal model with the mechanical model in order to obtain the fields of deformation and stress velocities.

III.2. Heat equation

Establishing the heat equation is based on the first principle of thermodynamics, which can be stated as follows: the total energy of an isolated system remains constant during its transformations. This can be mathematically expressed by the following laws:

Let M be a point in the flow and U be the specific internal energy at that point.[7]

$$\rho \frac{du}{dt} = -\text{div } q + \sigma \dot{\bar{\varepsilon}} \quad \text{(III.5)}$$

Where $\sigma_0 \underline{\underline{(\cdot)}}_s$ represents the plastic power transformed into heat according to the Hollomon law, and q is the heat flux vector. Using Einstein's notation convention, we can write:

$$\text{Div } q = \frac{\partial q_i}{\partial x_i} \qquad \text{(III.6)}$$

with $i \llbracket 1 ; 3 \rrbracket$, Fourier's law gives:

$$q_i = -\lambda \frac{\partial T}{\partial x_i} \text{ soit } q_i = -\lambda \text{grad } T \qquad \text{(III.7)}$$

It is assumed that U depends primarily on temperature and the equivalent Von Mises strain. Since U = U(T, $\bar{\varepsilon}$), we have:

$$\frac{du}{dt} = \frac{\partial u}{\partial T}\frac{dT}{dt} + \frac{\partial U}{\partial s}\frac{ds}{dt} \qquad \text{(III.8)}$$

we have $c = \frac{du}{dT}$; where c is the thermal conductivity of the material and $\underline{\underline{\cdot}}_s = \frac{d\underline{\underline{s}}}{dt}$

Then the equation (III.5) is written:

$$\rho \left[c \frac{dT}{dt} + \underline{\underline{\delta u}}_s \right] = div\, q + \sigma \underline{\underline{\cdot}}_s \qquad \text{(III.9)}$$

$$\rho c \frac{dT}{dt} = (div\, \lambda\, grad\, T) + \underline{\underline{\cdot}}_s \sigma \left(1 - \frac{\rho}{\sigma} \frac{\partial u}{\partial s}\right) \qquad \text{(III.10)}$$

By making the approximation $(1-\frac{\rho}{\sigma}\frac{\partial u}{\partial \bar{s}}) = \Gamma^d = \text{cte}$.

The constant corresponds to the Taylor-Quinney coefficient. It is introduced because it is experimentally observed that only a fraction of the deformation work is used to heat the material. The remaining fraction $(1-\Gamma^d)$ is stored as defects in the crystal lattice.[1]

Γ^d is typically close to 0.9 (see Table I.1). Moreover, for the majority of metals, its exact value is not known.

We then obtain the heat equation during plastic deformation of the material considered:

$$\rho c \frac{dT}{dt} = \lambda \Delta(T) + \Gamma^d \sigma \underline{\underline{\cdot}}_s \qquad \text{(III.11)}$$

This equation is valid for all material elements undergoing plastic deformation; however, it is written in Lagrangian formulation.

To express this equation in Eulerian formulation, it is necessary to consider the partial derivative of temperature, whose decomposition is recalled below:

Let's consider a function F.[7]

$$dF=\frac{\partial F}{\partial t}dt+\frac{\partial F}{\partial x}dx+\frac{\partial F}{\partial y}dy+\frac{\partial F}{\partial z}dz \quad \text{(III.12)}$$

Hence the total derivative

$$\frac{dF}{dt}=\frac{\partial F}{\partial t}+\frac{\partial F}{\partial x}\frac{dx}{dt}+\frac{\partial F}{\partial y}\frac{dy}{dt}+\frac{\partial F}{\partial z}\frac{dz}{dt} \quad \text{(III.13)}$$
$$=\vec{u}.\vec{grad}(F)+\frac{\partial F}{\partial t}$$

When the steady-state regime is established, i.e., when $\frac{\partial F}{\partial t}=0$, the Eulerian equation of heat becomes:

$$\rho c\,\vec{u}\,\vec{grad}\,(T)=\lambda\Delta(T)+\Gamma^{d}\dot{\sigma}_{s} \quad \text{(III.13)}$$

It is this second equation, the Eulerian equation of heat in steady-state regime, that is used for solving our thermal problem. In fact, we choose a fixed reference frame of the rolling cylinders that "observes" the material flowing with a velocity field $\vec{u}$. It should be noted that this velocity field originates from the power minimization performed in [8]the method of streamline flow.

The thermal solution of the problem requires an iteration between this optimization of the velocity field and the calculation of the temperature field until they are compatible with each other, namely, thermal equilibrium is reached and minimal mechanical power is dissipated.

III.3. Finite Difference Method

If we are solely interested in thermal modeling, we can use the finite difference method, taking into account, if necessary, the velocity field experienced by the material in the particle derivative term of the temperature.[6]

The general equation of heat is expressed as follows:

$$\rho c\,\vec{u}\,\vec{grad}(T)=\lambda\Delta(T)+\Gamma^{d}\sigma_{0}\dot{}_{s} \quad \text{(III.14)}$$

That it can be written in this form:

$$\rho c\begin{pmatrix} u^{x}_{i;j} \\ u^{y}_{i;j} \end{pmatrix}.\begin{pmatrix} \frac{\partial T}{\partial x_{i;j}} \\ \frac{\partial T}{\partial y_{i;j}} \end{pmatrix}=\lambda\left[\frac{\partial^{2}T}{\partial^{2}x_{i;j}}+\frac{\partial^{2}T}{\partial^{2}T_{i;j}}\right]+\Gamma^{d}\sigma_{0}\dot{}_{s} \quad \text{(III.15)}$$

The principle of this method for solving this partial differential equation (PDE) is presented below.

$$\begin{cases} \Delta T + f = 0 \ sur \ \Omega \\ T = T^0 sur \ \Gamma_1 \\ \frac{\partial T}{\partial n} = g \ \Gamma_2 \end{cases}$$

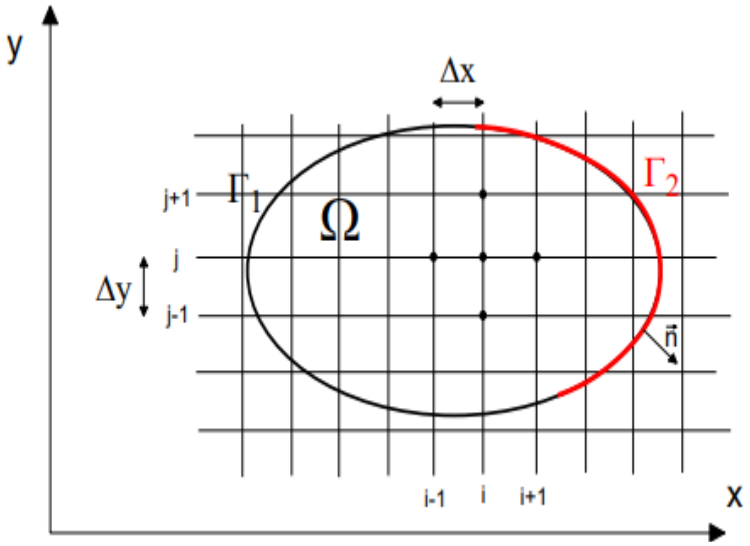

Figure III.1. Principle of finite differences [2]

III.4. Finite Difference Modeling

III.4.1 Introduction

The thermal problem is highly nonlinear and too complex to be treated and solved purely analytically. In practice, most of the equations to be solved are first or second-order equations with two independent variables. If T is a function of x and y, then the PDEs involve

$\frac{\partial T}{\partial x}$; $\frac{\partial T}{\partial y}$; $\frac{\partial^2 T}{\partial x}$; $\frac{\partial^2 T}{\partial y}$; $\frac{\partial^2 T}{\partial x \partial y}$III.1 Finite Difference Modeling.

The thermal problem is highly nonlinear and too complex to be treated and solved purely analytically. In practice, most of the equations to be solved are first or second-order equations with two independent variables. If T is a function of x and y, then the partial differential equations involve...

Therefore, to solve partial differential equations, a commonly applied method is the finite difference method. This method is used to approximate spatial derivatives in steady-state regime. The problem is considered two-dimensional (2D), in a plane containing the rolling direction (RD) and the normal direction (ND).[3]

III.5. Meshing

A mesh is applied to the domain under study. In order to simplify the expression of the temperature gradient, the angle formed by the lines with respect to the horizontal is neglected (assuming it is close to 0, see Figure III.2.2). This assumption becomes stronger as the reduction ratio increases. Calculations are detailed to account for the inclination of the trajectories.

The velocity fields of the material elements during their passage between the cylinders are known. The aim is to estimate the temperature field at any point in the rolling mill during steady-state operation. The only unknown quantity is the temperature at each point.[7]

III.6. Boundary Conditions

Boundary conditions are the values of the solutions of ordinary differential equations and partial differential equations on a boundary. There are many possible boundary conditions depending on the problem formulation and the number of variables involved. For volume nodes, the heat equation (III.10) is applied, but for surface nodes, different boundary conditions are applied, which are represented in Figure III.2.3 and detailed in the following paragraph:

The surface Σ_1 represents the nodes at the entry of the rolling mill. It is assumed that the material velocity is sufficiently high for the node temperature to be equal to the initial plate temperature. This surface is delimited by $1 \leq i \leq Imax$ and $j = 1$.[5]

The surface Σ_2 represents the nodes in contact with the upper cylinder. On this surface, there is a heat exchange due to plastic deformation. There is also heat generated by the friction between the cylinder and the plate, which is shared between them (details of this sharing are provided in the following paragraph). This surface is delimited by $2 \leq j \leq Jmax$ and $i = 1$.

The surfaces Σ_3, Σ_4, Σ_5 represent the nodes in contact with the air after the plate exits the rolling mill. Generally, this is the cooling phase of the plate. It is assumed that the air is at ambient temperature. These surfaces are delimited by $\Sigma_3 \Rightarrow Imax+1 \leq j \leq Imax+Mmax$ and $i = 1$, $\Sigma_4 \Rightarrow 2 \leq i \leq Imax-1$ and $j = Imax+Jmax$, and $\Sigma_5 \Rightarrow Imax+1 \leq j \leq Imax+Mmax$ and $i = Imax$.

The surface Σ_6 is similar to surface Σ_2, but it represents the nodes in contact with the lower cylinder. The exchanges on this surface are of the same type as those on Σ_2. This surface is delimited by $2 \leq j \leq Jmax$ and $i = Imax$.

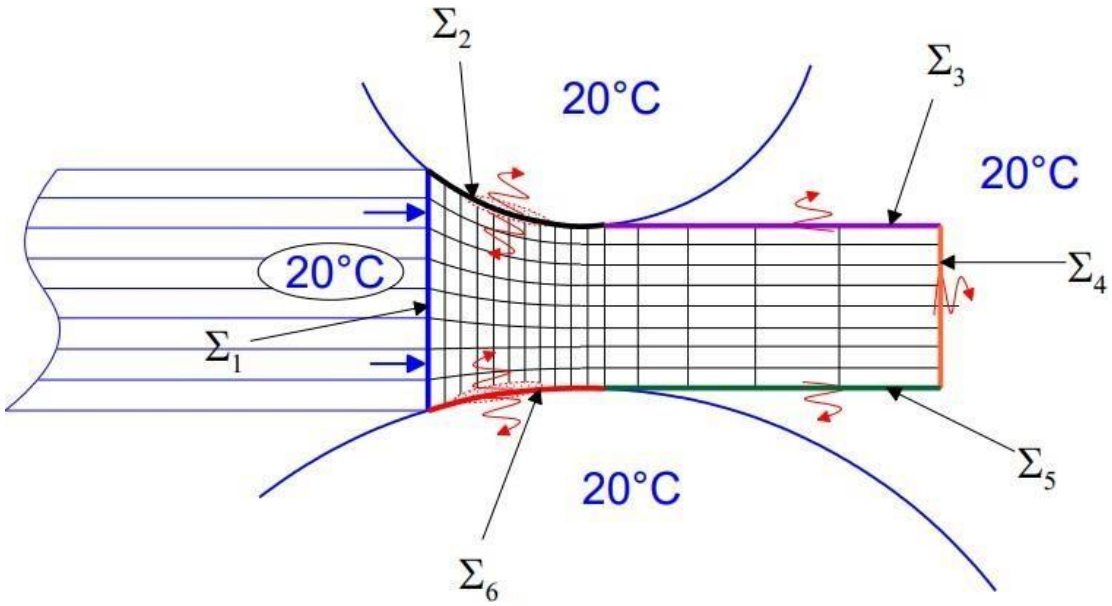

Figure III.2.Mapping of boundary conditions [11]

As mentioned in the above paragraph,[10] the heat generated by friction between the cylinder and the plate is shared between these two bodies. To evaluate this heat flux quantity, a local balance is performed using the boundary layer formulation. The heat flux, denoted as , is equal to the surface power dissipated by friction.

$$\Phi = w_F = \int_0^L \bar{m} \frac{\sigma}{\sqrt{3}} |\Delta V| dl \qquad \text{(III.16)}$$

The plate and the cylinders have a given temperature. During rolling, the heat generated by friction will be diffused into both contacting bodies. Therefore, it is necessary to determine the heat flux Φ_{tole} and Φcyl that is diffused into each body, knowing that $\Phi=\Phi_{tole}+\Phi cyl$. In general, the heat diffusion in a semi-infinite solid body from the surface can be represented as shown in Figure III.2.1.[4]

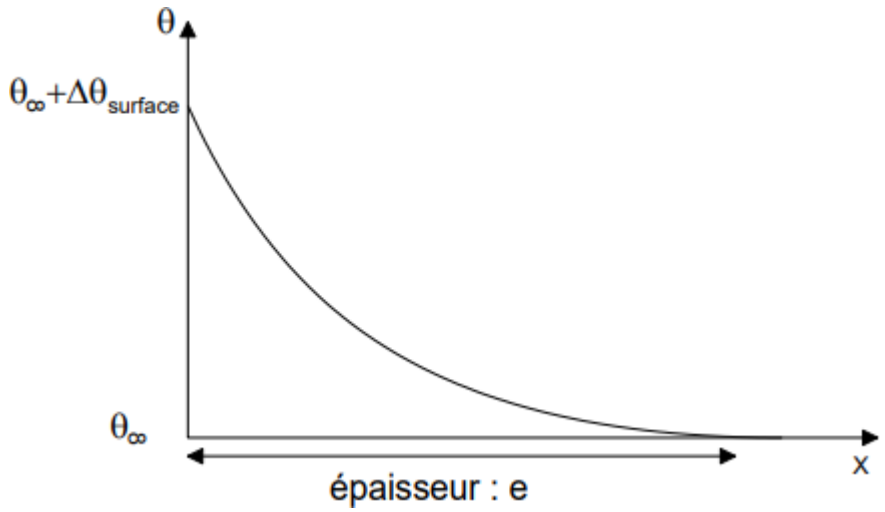

Figure III.2.1 Heat diffusion in a semi-infinite massive body from the surface [4]

The heat flow that passes through the surface is thus written:

$$\Phi = -\lambda\left(\frac{d\theta}{dx}\right) = 2\lambda\left(\frac{\theta_s - \theta_i}{e}\right) = 2\lambda\frac{\Delta\theta_s}{e} \qquad \text{(III.17)}$$

For the plate, by calculating the change in internal energy of a strip of width dx and thickness e_{tole}, we obtain:

$$\frac{1}{3}\rho_{tole} c_{tole} \Delta\theta_s \, e_{tole} = \int_0^t \Phi_{tole} dt \qquad \text{(III.18)}$$

By multiplying both sides by... $2\lambda_{tole}\frac{\Delta\theta_s}{e_{tole}}$, we obtain:

$$\frac{2}{3}\lambda_{tole}\rho_{tole}c_{tole}(\Delta\theta_s)^2 = \frac{2\lambda_{tole}(\Delta\theta_s)}{e_{tole}} \int_0^t \Phi_{tole} dt = \Phi_{tole}\int_0^t \qquad \text{(III.19)}$$

With b_{tole} being the thermal effusivity of the material, which characterizes its ability to exchange thermal energy with its surroundings.

III.2.4 Discretization

III.2.4.a Discretization of the heat equation in the volume[6]

Recalling the heat equation (III.22), it is discretized as follows for the volume elements:

$$2 \le i \le Imax - 1; 2 \le j \le Jmax + Mmax - 1$$

$$\rho c\vec{u}\, grad\vec{d}(T) = \lambda\Delta(T) + \Gamma_d\sigma_0 c^{\cdot} \qquad \text{(III.20)}$$

Which we can write in this form:

$$\rho c.\left(P^{x}_{i,j}\right).\left(\frac{\partial T}{\partial x}_{i,j}\right) = \lambda\left[\frac{\partial^2 T}{\partial x^2}_{i,j} + \frac{\partial^2 T}{\partial^2 y_{i,j}}\right] + \Gamma_d \sigma_0 c \quad \text{(III.21)}$$

$$\rho c\left[P^{x}_{i,j}\ \frac{T^{(i;j+1)} - T^{(i;j-1)}}{2\Delta x} + P^{x}_{i,j}\ \frac{(T^{i;j+1} - T^{i;j-1})}{2\Delta y}\right] \quad \text{(III.22)}$$

$$= \lambda\left[\frac{T^{(i;j+1)} - 2T^{(i;j)} + T^{(i;j-1)}}{\Delta x^2} + \frac{T^{(i;j+1)} - 2T^{(i;j)} + T^{(i;j-1)}}{\Delta y^2}\right] + \Gamma_d \sigma_0 c$$

After factoring, we have:

$$\left(\frac{\rho c P^{x}_{i,j}}{2\Delta y} - \frac{\lambda}{\Delta y^2}\right) T_{i;j-1}(A) + \left(\frac{\rho c P^{y}_{i,j}}{2\Delta y} - \frac{\lambda}{\Delta y^2}\right) T_{i;j+1}(B) \left(-\frac{\rho c P^{x}_{i,j}}{2\Delta x} - \frac{\lambda}{\Delta x^2}\right) T_{i;j-1}(C)$$

$$+\left(\frac{\rho c P^{x}_{i,j}}{2\Delta x} - \frac{\lambda}{\Delta x^2}\right) T_{i;j+1}(D) + \frac{2\lambda}{\Delta x^2} + \frac{2\lambda}{\Delta y^2}\ T_{ij}\ (E) = \Gamma_d \sigma_0 c \quad \text{(III.23)}$$

Now, we need to discretize the second term Γ_d σ_0ε. But first, we need to define the flow law used in our model. In order to accurately describe the physical phenomena that occur in the sheet during hot or cold rolling, it is necessary to have a law that can take into account:

- Viscoplastic behavior when modeling hot rolling.[6]
- Work hardening in the case of cold rolling.
- or an elastoplastic behavior if we want to simplify the problem.

In our case, we choose a power law (Hollomon's law):

$$\sigma_0 = \sigma^1 + k\varepsilon^n \dot{\varepsilon}^m \exp\left(\frac{mQ}{RT}\right) \quad \text{(III.24)}$$

With σ₁, s, and k being two constants, n is the work hardening coefficient which is approximately 0.2-0.5, analogous to the case of cold deformation, m is the sensitivity coefficient to strain rate and is approximately 0.1-0.3-0.5 for superplastic alloys, Q is the apparent activation energy (see Table III.1). n, m, and Q are intrinsic material parameters determined through rheological tests. R is the gas constant, and T is the absolute temperature.[1]

	Q mise en forme ($\dot{\bar{\varepsilon}}$ élevée)	Q fluage ($\dot{\bar{\varepsilon}}$ faible)	Q autodiffusion
Aluminium (Restauration dynamique)	155	138-150	138
Fer α (Restauration dynamique)	276	284	238-280
Cuivre (Recristallisation dynamique)	301	196-234	184-234
Fer γ (Recristallisation dynamique)	280	255	272-309

Tableau III.2 Energie d'activation apparente en (kJ /mole)[8]

This law is widely used for the hot behavior of aluminum alloys. It has the advantage of relating the main thermomechanical quantities to each other. Furthermore, the rheological parameters of this law can be easily identified through standard mechanical tests.

Discretization of the constitutive law.[9]

$$\Phi = \Gamma \quad \cdot = \Gamma \quad {}^{1} \quad \cdot \quad {}^{mQ}) \qquad \text{(III.25)}$$

$$_{d\sigma_0}\ \bar{}_{s} \quad _{d}\ \sigma_0 = \sigma \ + k\varepsilon\ \varepsilon^{n}\ \bar{}_{s}^{m} \exp\ (\frac{}{RT}$$

$$\Gamma \quad \dot{} \quad \bar{} \quad \cdot\!+\Gamma_d k s^{-n} \ldots^{m+1} \quad \frac{mQ}{RT^0} \quad \exp(1+\frac{mQ}{RT^0}) -$$

$$_{d\sigma_0} \quad \cdot_{\varepsilon} = \Gamma_{d\sigma} \qquad \bar{}_{s} \qquad \exp(\qquad \text{(III.26)}$$

$$\Gamma_d k\varepsilon^{-n}\ \dot{}\ \bar{}_{s}^{m+1} \exp\ (\frac{mQ}{RT^0})\ \exp\ (1 + \frac{mQ}{RT^{2^0}})\ T_{ij}$$

For any node of the index volume ($_i$, $_j$)$2 \leq i \leq Imax\ et\ 2 \leq j \leq Jmax + Mmax_1$

$$A_{ij}\ T(_i - _j\ ) + B_{ij}\ T(_i{}^{+}{}_j\ ) + C_{ij}\ T(_{ij}\ {}^{-}) + D_{ij}\ T(_{ij}\ {}^{+}) + (E'_{ij}\ + E'')T_{ij} \qquad \text{(III.26)}$$

Avec:

$A_{ij}= -(\frac{\rho c P^{x}}{2\Delta y}{}_{i,j} - \frac{\lambda}{\Delta y^2})$;$B_{ij}= (\frac{\rho c P^{y}}{2\Delta y}{}_{i,j} - \frac{\lambda}{\Delta y^2})$

$C_{ij}=-(\frac{\rho c P^{x}}{2\Delta x}{}_{i,j} - \frac{\lambda}{\Delta x^2})$; $D_{ij}=(\frac{\rho c P^{x}}{2\Delta x}{}_{i,j} - \frac{\lambda}{\Delta x^2})$

$E_{ij}= (\frac{2\lambda}{\Delta x^2} + \frac{2\lambda}{\Delta y^2}) + \Gamma_d k\varepsilon^{\ n}\ \bar{}_{s}^{m} - \ \cdot^{m+1} (\frac{mQ}{RT^{2^0}}) \exp (\frac{mQ}{RT^0})$

$Q(T_0)=\Gamma_d\ k\varepsilon^{-n}\ \dot{}\ \bar{}_{s}^{m+1} \exp\ (\frac{mQ}{RT^0})\ \ (1 + \frac{mQ}{RT^{2^0}})$

III.2.4.b Discretization of boundary conditions

To better understand the[3] boundary conditions, let's refer back to Figure III.2.3. Boundary condition on Σ_l:

For $1 \leq i \leq Imax$ and $j = 1$, the discretized boundary condition on Σ_l is:

$$T(_{i,1})=T_{in} \qquad (III.27)$$

Boundary condition on Σ_2:

For $2 \leq j \leq jmax$ and $i = 1$, the boundary condition on Σ_2 is:

$$\frac{T(^{1}_{j})-T(^{2}_{,j})}{\frac{b_t \ _o Le}{\Delta y}} = \frac{1}{\lambda}\left(-h(T(^{1}_{j}) - T)\frac{\qquad}{b_t \ _o Le+bcs}\right) w_{\ 1}) \qquad (III.28)$$

$$F$$

For $Imax+1 \leq j \leq Imax + Mmax$ and $i = 1$, the boundary condition on Σ_3 is:

$$\frac{(T(^{1}_{j})-T(^{2}_{,j})}{\Delta y} = -\frac{h_{air}}{\lambda}(T(^{1}_{,j})\text{-Tair} \qquad (III.29)$$

Condition aux limites sur la Σ_4 :

For $2 \leq i \leq imax-1$ and $j= Imax+Jmax$, the boundary condition on Σ_4 is:

$$\frac{T(i,Mmax+jmax)-T(i,Mmax+jmax-1)}{\Delta y} = \frac{h_{air}}{\lambda}(T(imax,j) - T_{air}) \qquad (III.30)$$

To refine the finite difference calculation result, the boundary conditions can be approximated by local quadratic functions. The temperature field is approximated by a parabola (ax^2bx c) at the nodes (1,j),(2, j) (3,j)$\forall$ jϵ2, jmax and in contact with the upper cylinder, and the nodes (Imax-2,j),(Imax-1,j) (Imax, j) , max and in contact with the lower roll. At the nodes (1,j),(2,j) (3,j)$\forall j\epsilon$ 2,j max and [7] , the parabola is centered at(1, j) and the term b of the parabola is not zero because the temperature derivative does not vanish at the boundary condition at(1,j) leading to a more general expression.

$$a\Delta y^2+b\Delta y + T(3,j) = T(2,j) \qquad (III.31)$$

:

-

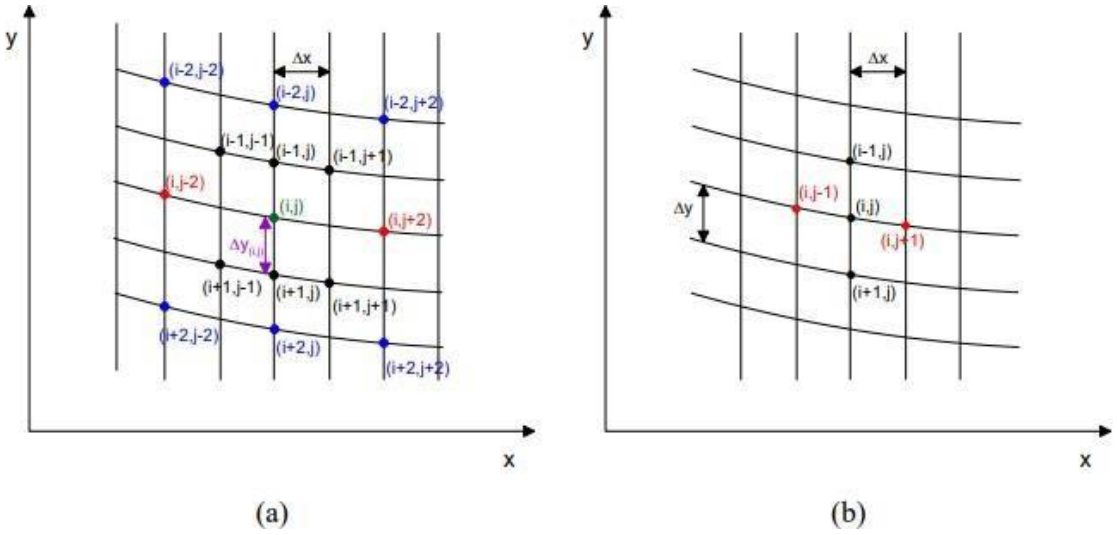

Figure III.2.2 calculation nodes; (a) calculation closer to reality (b) approximate calculation

[5]Figure III.2.3 (a) represents all the nodes involved in the calculation for a single equation, while Figure III.2.6 (b) represents the nodes of the first calculation. The second calculation is very complex as it requires a lot of solving time and does not necessarily yield more significant results than the first calculation. That is why it is not implemented in the modeling of rolling for a viscoplastic material.

Table des matières

CHAPTER IV : RESULTS AND COMMENTS

IV .1.Rolling Mill Data

For different parameters in each case, an asymmetric rolling pass was simulated (including the symmetric case). Only the working rolls and the sheet were considered in this modeling. The sheet has an input thickness of 20 mm. In a rolling pass, it undergoes a 20% reduction in thickness, resulting in an output thickness of 16 mm from the rolling mill. The rolls have the same radius of 100 mm. The upper roll has an angular velocity of 1.57 rad/s to achieve a tangential velocity of 157 mm/s. The lower roll has the same diameter but its velocity is variable with a maximum speed of 1.57 rad/s. The rolls are considered undeformable.

We neglected transverse deformations (2D modeling), which allowed us to simplify the model by assuming plane strain.

IV .2.Thermal Data

Thermal effects occur at various levels during the rolling simulation, and the following temperatures are considered:
Temperature of the upper roll: T_cylsup (constant in steady state)
Temperature of the lower roll: T_cylinf (constant in steady state)
Air temperature : T_air (constant)
Sheet temperature: T_tole (constant)

Additionally, during plastic deformation, the material locally heats up. In addition to that, there is energy dissipated by friction in the friction zone. Therefore, it is necessary to manage the heat exchange between all these different parts. We introduce the following heat exchange parameters:
- Band-air heat exchange: h_air = 25 W/(m^2·K)
- Band-upper roll heat exchange: h_cs = 10 kW/(m^2·K)
- Band-lower roll heat exchange: h_ci = 25 W/(m^2·K)
- Friction energy partition coefficient: b = b_total/(b_cyl + b_tole) = 0.5 (i.e., a portion of the energy dissipates in the band, the other portion in the roll in contact with the same proportion). b_tole and b_cyl are the thermal effusivities of the sheet material and roll material, respectively. They are characterized by their capacity to exchange thermal energy with their surroundings.

It should be noted that finely adjusting these parameters to reproduce real-world conditions is very challenging. These parameters vary depending on the rolling time, number of passes, and other factors. The assumed temperatures at the beginning of each pass are kept constant throughout the pass.

IV .3.Thermal parameters:

Density (ρ): 2700 kg/m^3

Specific heat capacity (C_P): 897 J/(kg·K)

Thermal conductivity (λ): 237 W/(m·K)

T_cylsup = T_cylinf = T_tole = T_air = 293 K

The thermal aspect of asymmetric rolling has been studied. For the process modeling, we adopted two numerical methods, finite differences and finite volumes, due to its complexity. The thermal model developed using finite differences was compared to the results obtained using finite volume calculations with the **Gambit** and **Fluent software**.

IV .4.Solution

Methods a- Finite

Differences

The thermal problem is highly nonlinear and too complex to be treated and solved purely analytically. In practice, most of the equations to be solved are first or second-order partial differential equations with two independent variables. To solve partial differential equations, a commonly applied method is the finite difference method. This method is used to approximate spatial derivatives in steady-state conditions. The problem is considered two-dimensional (2D), in a plane containing the rolling direction (RD) and the normal direction (ND).

We have developed a program in Matlab that allows us to determine the thermal field at any point on the strip (sheet), given the thermal parameters.

a-

```
% Define parameters
lambda_tole = 237; % Thermal conductivity of the sheet (W/m.K)
dx = 0.06; % Grid spacing in the x-direction (mm)
dy = 0.02; % Grid spacing in the y-direction (mm)

% Define grid size and dimensions
N = 100; % Number of grid points in x-direction
M = 100; % Number of grid points in y-direction

% Initialize temperature matrix
T = zeros(M, N);
T(:, 1) = 293; % Initial temperature on the left boundary
T(:, end) = 293; % Initial temperature on the right boundary

% Perform finite difference iterations
max_iter = 1000; % Maximum number of iterations
tolerance = 1e-6; % Tolerance for convergence
```

```
for iter = 1:max_iter
    T_prev = T; % Store previous iteration

    % Update temperature at interior points using finite difference method
    for i = 2:N-1
        for j = 2:M-1
            T(j, i) = (T_prev(j, i-1) + T_prev(j, i+1) + T_prev(j-1, i) + T_prev(j+1, i)) / 4;
        end
    end

    % Check convergence
    if max(abs(T(:) - T_prev(:))) < tolerance
        break;
    end
end

% Create coordinate grids for plotting
```

```
% Create coordinate grids for plotting
x = linspace(0, 60, N);
y = linspace(-10, 10, M);
[X, Y] = meshgrid(x, y);

% Plot the temperature field
figure;
contourf(X, Y, T', 'LineWidth', 1);
colorbar;
xlabel('x (mm)');
ylabel('y (mm)');
title('Temperature Field (c)');
```

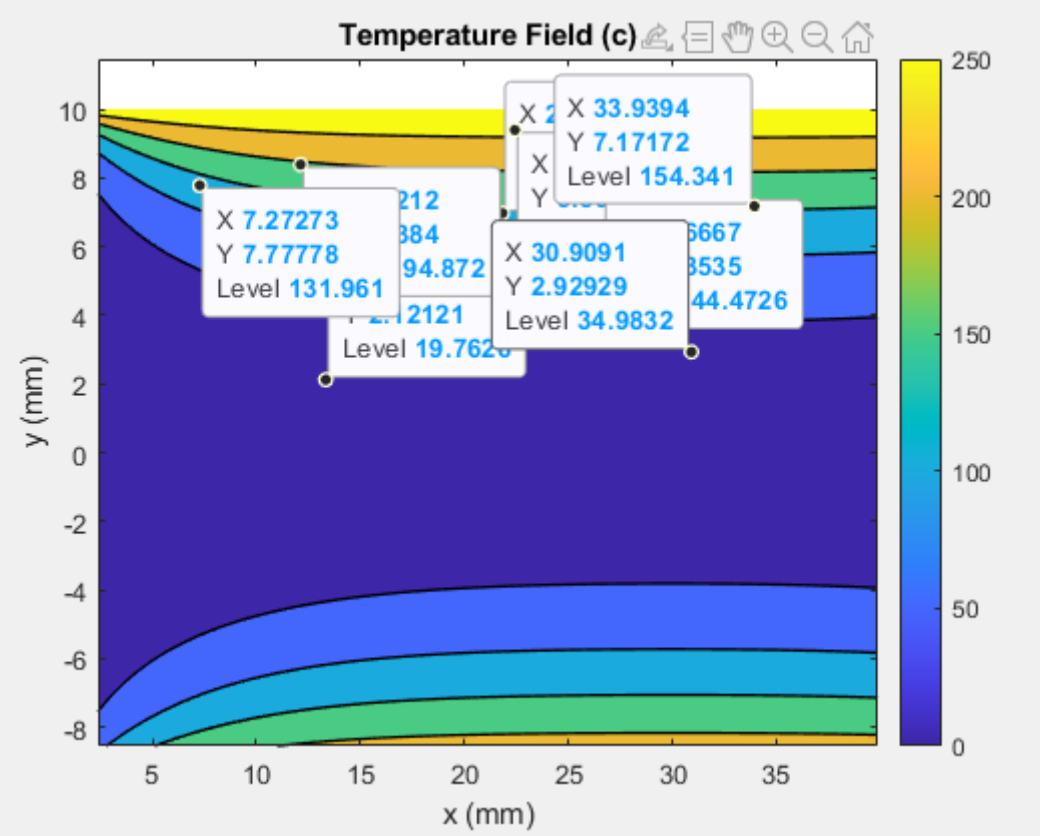

Figure IV.1 Temperature field with friction consideration

b- Finite Volume Methods

The finite volume method is a numerical approach used to solve partial differential equations. This approach is characterized by representing the field in specific volume units rather than sporadic points, similar to the finite difference method.

In the finite volume method, the field is divided into a set of limited sizes, also known as cells or elements. Partial differential equations are integrated over each limited size using an appropriate approximation of the solution. Mass fluxes, mobility, and energy between cell interfaces are also considered to ensure the preservation of physical quantities.

This method offers several advantages, including:

Conservation: The finite volume method ensures the conservation of physical quantities such as mass, momentum, and energy across cell interfaces.

Engineering Flexibility: It can be applied to complex and unstructured engineering using irregular grids.

Numerical Stability: The finite volume method is naturally stable and effectively handles changing phenomena and numerical instability.

By using software such as Gambit and Fluent, volumetric grids can be set up and problems can be analyzed using the finite volume method, providing accurate results for thermal fluxes and distribution within the panel.

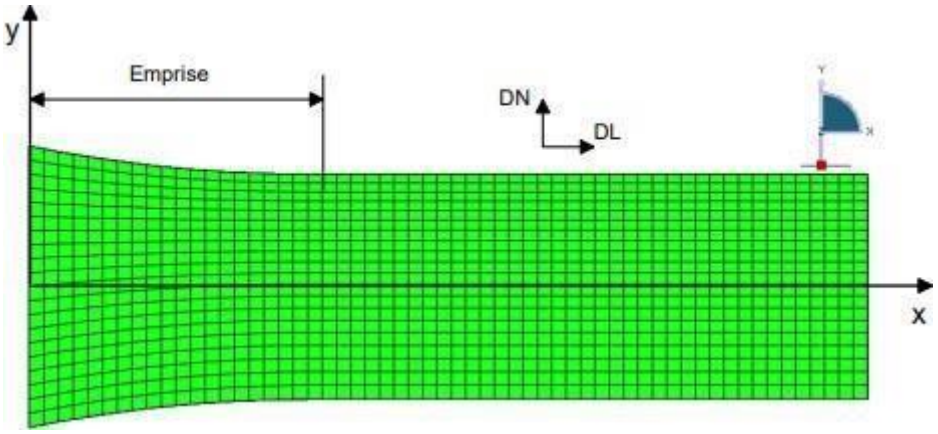

Figure IV.2 Plate mesh

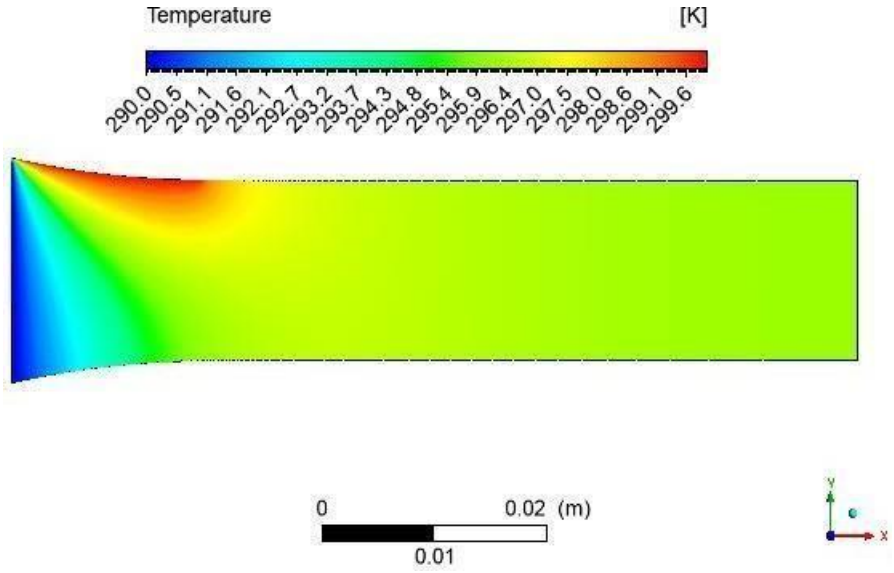

Figure IV.3 Temperature field with friction consideration

IV .5.Interpretations of results

(i) The thermal modeling conducted using both methods in this chapter appears to be generally valid. It is observed that the finite difference method yielded results, while the finite volume method produced less accurate results due to neglecting the curvature of trajectories.

(ii) The finite difference method is more valid when the reduction ratios are low, the sheets are thin, and the cylinders are larger.

(iii) With the finite difference method, we were able to study viscoplastic materials by incorporating them into our trajectory model.

(iv) For the thermal aspect, the finite volume method is a relevant tool for validating the finite difference method.

(v) The obtained results are consistent with expectations, indicating that friction has a dominant effect and that the temperature is higher on the side of the faster cylinder.

General Conclusion

Rolling presents a wide range of thermal problems. It starts with the reheating furnaces for hot rolling, where we must ensure, while using the least amount of energy possible, the temperature homogeneity so that the product can be rolled at the most uniform temperature.

The objective of this work was the thermal modeling of asymmetric rolling, focusing on its thermal aspect. For the process modeling, we adopted two numerical methods, finite differences and finite volumes. The temperature field predictions were compared to the results obtained through finite volume calculations using Gambit and Fluent software.

From this study, the following conclusions can be drawn:

(i) It is observed that the finite volume method provided more accurate results compared to the finite difference method, where we neglected the curvature of the trajectories.

(ii) The finite difference method is more valid when the reduction ratios are low, and when dealing with thin sheets and large cylinders.

(iii) Using the finite difference method, we were able to study viscoplastic materials by introducing them into our trajectory model.

(iv) For the thermal aspect, the finite volume method is a relevant tool for validating the finite difference method.

(v) The obtained results are consistent with expectations, showing that friction effects are predominant and that the temperature is higher on the side of the faster cylinder.

Finally, the application of the model was presented in Chapter IV..

BIBLIOGRAPHY

CHAPTER I :

[1] YUN (I.S.), WILSON (W.R.D.), EHMANN (K.F.). – Review of chatter studies in cold rolling. Int. J. Mach. Tools & Manuf. 38 (1998), 1499-1530.

[2] VATNE (H.E.), MARTHINSEN (R.), ØRSUND (R.), NES (E.). – Modelling recrystallization kinetics, grain sizes and textures during multipass hot rolling. Met. Mat. Trans. A 27A (1996), 4133-4144.

[3] PIETRZYK (M.), KEDZIERSKI (Z.), KUSIAK (H.), MADEJ (W.), LENARD (J.G.). – Evolution of the microstructure in the hot rolling process. Steel Research 64, 11 (1993), 549-556.

[4] KARHAUSEN (K.), KOPP (R.), DE SOUZA (M.M.). – Numerical simulation method for designing thermomechanical treatments, illustrated by bar rolling. Scand. J. Met. 20 (1991), 351-363.

[5] NOAT (P.). – Détermination expérimentale et prise en compte dans un code de calcul par éléments finis de l'anisotropie mécanique d'alliages d'aluminium laminés. Thèse de Doctorat en Science et Génie des Matériaux, École des mines de Paris (1996).

[6] DENIS (S.). – Prévision des contraintes résiduelles induites par traitements thermiques et thermochimiques. Rev. Mét. CIT/Sc. Génie Mat. 2 (1997), 157-176.

[7] COLONNA (F.). – Modélisation numérique du refroidissement des rails. Thèse de Doctora en Science et Génie des Matériaux, École des mines de Paris (1992).

[8] CHENOT (J.-L.), MONTMITONNET (P.), BERN (A.), BERTRAND-CORSINI (C.). – A method for determining free surfaces in steady state finite element computations. Comp. Meth.Appl. Mech. Eng. 92, 2 (1991), 245-260.

[9] SLUZALEC (A.). – Simulation of stochasticmetal forming process for rigid-viscoplastic material. Int. J. Mech. Sci. 42 (2000), 1935- 1946.

[10] GAVRUS (A.), MASSONI (E.), CHENOT (J.-L.). – Identification du comportement rhéologique par analyse inverse. Revue Européenne des Eléments Finis, vol. 7, n° 1-2-3 (1998), 23- 38.

[11] WAGONER (R.H.), CHENOT (J.-L.). – Metal Forming Analysis. Cambridge University Press (2001).

[12] MONTMITONNET (P.), WEY (E.), DELAMARE (F.), CHENOT (J.L.), FROMHOLZ (C.), DE VATHAIRE (M.). – A mechanical model of cold rolling. Influence of the friction law on roll flattening calculated by a Finite Element Method. Proc. 4th Int. Steel Rolling Conf. (Deauville, 1987). Publié par IRSID/ATS.

[13] BROOKS (A.N.), HUGHES (T.J.R.). – Streamline Upwind / Petrov-Galerkin formulations for convection-domi

[14] CHENOT (J.-L.). – Méthodes de calcul en plasticité. M 595 (1991)

CHAPTER II:

[1] IRVINE (K.J.), PICKERING (F.B.) et GLADMAN(T.). – JISI 205, p. 161 (1967).

[2] LESLIE et al. – Trans. Am. Soc. Met. 46, p. 1 470 (1954).

[3] NARITA. – Transaction ISIJ 15, p. 145 (1975).

[4] MCQUEEN (H.J.) et JONAS (J.J.). – *in Treatise on materials science and technology,* vol. 6. Édité par Arsenault (R.J.) Academic Press, New York, p. 393.

[5] TEGART (W.J.). – in *Recrystallization 92.* Éds Fuentes et Gil Sevillano. San Sebastian, Trans. Tech. Publications p. 1.

[6] JONAS (J.J.). – in *Mathematical modelling ofhot rolling of steel.* Proceeding of the Interna-tional Symposium in Hamilton, edited by S. Yue, p. 99 (1990).

[7] YAMAMOTO (S.) et col. – Proc. of *Thermome- chanical processing of microalloyed auste- nite,* Pittsburgh, p. 613 (1981).

[8] SELLARS (C.M.). – in *Thermec 88,* Tokyo, p. 448 (1988).

[9] CHOQUET (P.) et col. – in *Mathematical modelling of hot rolling of steel.* Proceeding of the International Symposium in Hamilton, édité par S. Yue, p. 34 (1990).

[10] JONAS (J.J.) et WEISS (I.). – Metal Science, p. 238 (1979).

[11] LE BON (A.) et col. – Metal Science, vol. 9, p. 36 (1975).

[12] MCQUEEN (H.J). – in *Recrystallization 92.* Éds Fuentes et Gil Sevillano. San Sebastian, Trans. Tech. Publications, p. 429.

CHAPTER III:

[1][Akbari Mousavi et al., 2007] S.A.A. Akbari Mousavi, S.M. Ebrahimi et R. Madoliat, Three dimensional numerical analyses of asymmetric rolling. J. Mater. Proc. Technol., vol. 187-188, pp. 725–729, 2007.

[2][Asbeck et Mecking, 1978] H. Asbeck et H. Mecking, Influence of friction and geometry of deformation on texture inhomogeneities during rolling of Cu single crystals as an example. Mater. Sci. Eng., vol. 34, pp. 111–119, 1978.

[3][Bacroix et Jonas, 1988] B. Bacroix et J. J. Jonas, The Influence of non-octahedral slip on texture development in FCC metals. Textures and Microstructures, vol. 8 & 9, pp. 267-311, 1988.

[4][Baque et al., 1973] P. Baqué, E. Felder, J. Hyafil et Y. D'Escatha, Mise en forme des

métaux, calcul par la plasticité (tome 1), 1973.
[Baque et al., 1973] P.Baque, E.Felder, J.Hyafil et Y.D'Escatha, Mise en forme des
[5]métaux, calcul par la plasticité (tome 2), 1973.
[Bataille, 2003] C. Bataille, Laminage des produits longs - Définitions et paramètres.
[6]Techniques de l'ingénieur, M7900, 2003.
[Beynon, 1998] J. Beynon, Tribology of hot metal forming. Tribology International,
vol. 31, pp. 73–77, 1998.
[7][Bunge et Esling, 1997] H. Bunge et C. Esling, Texture et anisotropie des matériaux.
Techniques de l'Ingénieur, vol. M605, 1997.
[8][Bunge, 1982] H. Bunge, Texture Analysis in Materials Science. Buttherworth,
London, 1982.
[9][Buxton et Browning, 1972] S.A. Buxton et S.C. Browning, Turn-up and turn-down in
hot rolling: a study on a model mill using plasticine, J. Mech. Eng. Sci., vol. 14,
pp. 245□254, 1972.
[10][Chekmarev et al., 1956] A.P. Chekmarev et A.A. Nefedov, Obrabotka Metallov
Davleniem, vol. 4(2), (British Library Translation R.T.S. 8939), 1956.
[11][Chenot, 1991] J.L. Chenot, Méthodes de calcul en plasticité, Techniques de
l'ingénieur. M 595, 1991.